AD_____

Award Number DAMD17-93-V-3013

TITLE: Neural Responses to Injury: Prevention, Protection and Research (Neuroscience Center of Excellence)

Subtitle: Role of Growth Factors and Cell Signalling in the Response of Brain and Retina to Injury

PRINCIPAL INVESTIGATOR: Nicolas G. Bazan, M.D., Ph.D.

CONTRACTING ORGANIZATION: Louisiana State University
New Orleans, Louisiana 70112-2234

REPORT DATE: October 1998

TYPE OF REPORT: Final

PREPARED FOR: U.S. Army Medical Research and Materiel Command
Fort Detrick, Maryland 21702-5102

REPORT DOCUMENTATION PAGE

Form Approved
OMB No. 0704-0188

1. AGENCY USE ONLY *(Leave blank)*	2. REPORT DATE	3. REPORT TYPE AND DATES COVERED
	October 1998	Final (20 Sep 93 - 19 Sep 98)

4. TITLE AND SUBTITLE
Neural Responses to Injury: Prevention, Protection and Research (Neuroscience Center of Excellence)

5. FUNDING NUMBERS
DAMD17-93-V-3013

6. AUTHOR(S)
Nicolas G. Bazan, M.D., Ph.D.

7. PERFORMING ORGANIZATION NAME(S) AND ADDRESS(ES)
Louisiana State University
New Orleans, Louisiana 70112-2234

8. PERFORMING ORGANIZATION REPORT NUMBER

9. SPONSORING / MONITORING AGENCY NAME(S) AND ADDRESS(ES)
U.S. Army Medical Research and Materiel Command
Fort Detrick, Maryland 21702-5012

10. SPONSORING / MONITORING AGENCY REPORT NUMBER

11. SUPPLEMENTARY NOTES
Subtitle: Role of Growth Factors and Cell Signalling in the Response of Brain and Retina to Injury

12a. DISTRIBUTION / AVAILABILITY STATEMENT
Approved for public release; distribution unlimited

12b. DISTRIBUTION CODE

13. ABSTRACT *(Maximum 200 words)*

14. SUBJECT TERMS
Prevention, Injury

15. NUMBER OF PAGES
87

16. PRICE CODE

17. SECURITY CLASSIFICATION OF REPORT	18. SECURITY CLASSIFICATION OF THIS PAGE	19. SECURITY CLASSIFICATION OF ABSTRACT	20. LIMITATION OF ABSTRACT
Unclassified	Unclassified	Unclassified	Unlimited

FOREWORD

Opinions, interpretations, conclusions and recommendations are those of the author and are not necessarily endorsed by the U.S. Army.

____ Where copyrighted material is quoted, permission has been obtained to use such material.

____ Where material from documents designated for limited distribution is quoted, permission has been obtained to use the material.

____ Citations of commercial organizations and trade names in this report do not constitute an official Department of Army endorsement or approval of the products or services of these organizations.

____ In conducting research using animals, the investigator(s) adhered to the "Guide for the Care and Use of Laboratory Animals," prepared by the Committee on Care and use of Laboratory Animals of the Institute of Laboratory Resources, national Research Council (NIH Publication No. 86-23, Revised 1985).

____ For the protection of human subjects, the investigator(s) adhered to policies of applicable Federal Law 45 CFR 46.

____ In conducting research utilizing recombinant DNA technology, the investigator(s) adhered to current guidelines promulgated by the National Institutes of Health.

____ In the conduct of research utilizing recombinant DNA, the investigator(s) adhered to the NIH Guidelines for Research Involving Recombinant DNA Molecules.

____ In the conduct of research involving hazardous organisms, the investigator(s) adhered to the CDC-NIH Guide for Biosafety in Microbiological and Biomedical Laboratories.

_____

PI - Signature Date

4- TABLE OF CONTENTS.

GENE EXPRESSION FOLLOWING ISCHEMIA-REPERFUSION AND TRAUMATIC BRAIN INJURY

5- INTRODUCTION

As a consequence of traumatic brain injury (TBI), ischemia, and seizures, neurotransmitters are released and, in turn, generate an overproduction of second messengers. A key player in excitotoxic neuronal damage is the excitatory amino acid, glutamate (Olney, 1986; Rothman and Olney, 1986; Choi, 1988), which is released and accumulates in brain after TBI (Faden et al., 1989; Katayama et al., 1990; Nilsson et al., 1990) and ischemia (Benveniste et al., 1984; Meldrum, 1990; Mitani et al., 1990; Christensen et al., 1991). Glutamate triggers increased permeation of calcium mediated by NMDA receptors and activation of many calcium-dependent signaling pathways. Calcium-mediated activation of PLA_2 and release of arachidonic acid (AA) are among the membrane lipid-derived signaling systems activated at the onset of these various forms of neurotrauma, which involve the over-release of neurotransmitters, the stimulation of post-synaptic receptors, and the subsequent accumulation of abnormally high concentrations of second messengers (Bazan et al., 1993; 1995).

In our laboratory as well as in others, research has focused on the generation of injury mediators linked to the activation of calcium-dependent PLA_2, the release of phospholipid-derived bioactive lipid molecules, including free AA and platelet-activating factor (PAF), and the signaling pathways activated as a consequence (Bazan et al., 1991; 1994; 1995; Bonventre, 1996; Farooqui et al.,1997). PAF, in turn, promotes the expression of early genes (c-*fos,* c-*jun,* Zif 268) and others acting as early genes, such as the inducible cyclooxygenase COX-2 (Marcheselli and Bazan, 1994; 1996). The activation of COX-2 (PGHS-2) leads to a delayed accumulation of prostaglandins that, either per se or through the free radicals generated during their synthesis, activate a cascade of events leading to DNA degradation and cell death through apoptosis (Bazan, 1997).

We, and others, have shown the neuroprotective properties of pharmacological agents targeting bioactive lipid signaling cascades. Detailed characterization of these processes, and the downstream events that link the over-accumulation of bioactive lipids to long-term changes in brain physiology, is important in identifying the best therapeutic targets for the treatment of brain injury.

Free AA may directly affect neuronal synaptic activity (Volterra et al., 1992) or can be further metabolized to prostaglandins (PG), leukotrienes (LT) and tromboxanes (TX) (Shimizu and Wolfe, 1990). These metabolites can not only modulate synaptic transmission (Piomelli, 1994), but can also affect the microvasculature: in PGs by affecting cerebral blood flow (Moncada and Vane, 1979) and in LTs by increasing the permeability of the blood-brain barrier

(Unterberg et al., 1987; Baba et al., 1991). The rate-limiting step in the biosynthesis of prostanoids (PGs and TXs) is the conversion of AA to PGH_2, a reaction catalyzed by cyclooxygenase (COX, prostaglandin G/H synthase, PGS). One of the most important recent findings in the cell biology of bioactive lipids is the discovery of a second isoform of the enzyme: COX 2 (Tis-10, PGS-2, inducible cyclooxygenase). Expression of the two isoforms is regulated in distinct ways. In most tissues, COX 1 is constitutively expressed, whereas COX 2 expression is stimulated by growth factors and cytokines, and displays a pattern of induction typical of the product of an immediate-early gene (Herschman, 1996). COX-2 and the constitutive COX-1 may contribute to eicosanoid production from free AA (Hershman, 1994), the latter under normal basal conditions and the former when synaptic activity is overstimulated (i. e. after ischemia, TBI, seizures).

The brain is one of the few sites in the body where COX 2 expression is detectable under resting conditions. This seemingly constitutive expression, which is localized in neurons, may be explained by activity-dependent induction in excitatory neurons (Yamagata et al, 1993). COX 2 immunoreactivity in brain has been noted in the post-synaptic structures of discrete sub-populations of excitatory neurons from cerebral cortex, hippocampus and amygdala (Kaufmann et al, 1996). Normal synaptic activity, specifically that involving the NMDA class of glutamate receptors, is sufficient to stimulate COX 2 expression (Yamagata et al, 1993). Therefore, the resting levels of COX 2 in brain can be accounted for by the proportion of excitatory neurons undergoing stimulation at any given moment.

COX 2 expression in the brain is also regulated by PAF (Bazan et al., 1994) and the pro-inflammatory cytokines released by astrocytes, microglia, and infiltrating inflammatory cells. COX 2 may, therefore, have a pivotal role at various stages of traumatic brain injury, including primary tissue damage, secondary inflammation and edema, recruitment of surrounding tissue into either degenerative or reparative processes, and the increased neuronal excitability associated with epileptogenesis.

Several lines of evidence point to a role for COX 2 in neuronal damage: (i) In ischemia-reperfusion (Collaco-Moraes et al, 1996) and in seizure models (Marcheselli and Bazan, 1994), COX 2 expression is up-regulated in those brain regions most vulnerable to damage; (ii) COX 2, but not transcription factor immediate-early genes, is more highly up-regulated in damaging versus non-damaging seizures; (iii) the specific COX 2 enzyme inhibitor, NS 398, reduces infarct volume in a model of focal ischemia-reperfusion (Nogawa et al, 1997). We and others have previously shown that COX 2 mRNA and protein are strongly up-regulated during several models of neurotrauma, including vasogenic brain edema (Bazan et al, 1995, and previous annual reports on this project) electroconvulsive shock (ECS), kainic acid (KA)-induced seizures (Marcheselli and Bazan, 1996), focal ischemia-reperfusion (Planas et al, 1995; Collaco-Moraes

et al, 1996), and spreading depression (Miettinen, 1997).

Activation of PLA_2 can stimulate the synthesis of platelet-activating factor (PAF), a mediator of inflammation and immune responses (Braquet et al., 1987) that has also been linked with ischemia/reperfusion-induced brain damage (Panetta et al., 1987). PAF actions are mediated through its interaction with receptors found extracellularly in presynaptic membranes and intracellularly in microsomal membranes (Marcheselli et al., 1990; Bazan et al., 1991). The PAF bioactivity toward the presynaptic receptors is to stimulate glutamate release, and the antagonist BN52021 blocks this effect (Clark et al., 1992). PAF, by interacting with intracellular binding sites, activates early gene transcription (c-fos, c-jun, zif-268, COX-2), and this effect is blocked by another PAF antagonist, BN50730 (Squinto et al., 1989; Bazan et al., 1991; 1995). BN 50730 also inhibits COX 2 induction in the ECS, KA and vasogenic edema models of brain trauma (Marcheselli and Bazan, 1996; Bazan et al, 1996). This suggests that PAF is synthesized as a result of $cPLA_2$ activation, such as in induction via NMDA receptor activation. This can influence downstream events in the injury/repair cascade by mechanisms that involve the activation of COX 2.

In this report, we further evaluate the early and late effects of cryogenic injury in gene expression, the increased expression of COX-2 in the ischemic core and penumbra of rat brain after ischemia-reperfusion, and the effect of the PAF antagonist BN50730. Because future studies will be done in transgenic mice (knockouts for PAF receptor and COX-2), we also developed and characterized a model of ischemia-reperfusion in mice. These animals models will further support the key roles of PAF and COX-2 in brain damage.

6- BODY.

Previous work.

In previous reports (**years 1-4**), we have shown that cryogenic injury to the brain leads to early changes in COX-2 expression and that PAF is involved in COX-2 induction and edema formation. Our results are summarized as follows:

1- Cryogenically-induced vasogenic brain edema in rats up-regulates COX 2 mRNA levels 2-3 hours post-injury, followed by a peak in COX 2 protein 4-5 hours after the injury and sustained for up to 24 hours.

2- PAF is involved in COX-2 activation and edema formation; the intracellular PAF receptor antagonist BN 50730 and the novel PAF antagonist LAU 503 block this induction and reduce blood-brain barrier breakdown.

3- Using electrophoretic mobility shift assays (EMSAs), we have shown that the DNA binding activities from rat brain nuclear extracts specific for AP2, CREB, GAS/ISRE and NFκB decrease during the cryogenic injury.

4- The COX-2 gene is modulated by a complex series of DNA binding proteins, in particular AP-2, NFκB and several yet unidentified regulatory elements that include a set of gene repressor proteins. Using a human B lymphoblast cell line (IM9) in which PAF treatment induces COX-2 transcription, we have shown that elevations in the protein-DNA binding of AP2 and NFκB immediately precede maximal COX-2 activation.

5- The PAF antagonist, BN50730, blocked PAF-induced COX-2 expression and the activation of transcription factors, AP2 and NFκB, in IM9 cells. This suggests that AP2 and NFκB are intimately linked with PAF-mediated COX-2 gene induction.

6- Utilizing DNA-magnetic bead affinity technology, we showed that one ~32-40 kDa DNA-binding protein, a non histone chromosomal protein (NHCP), may act as a COX-2 gene repressor and leave the COX-2 gene promoter region during the process of gene induction. We propose that removal of this NHCP protein from the COX-2 gene promoter may allow other positively activating transcription factors, such as NFκB, to bind in the place of, or near, this regulatory protein in order to activate transcription from the COX 2 gene locus.

7- We have shown that, although the rat and human COX-2 promoters show some differences in structure, the mechanisms by which PAF regulates their activity appear to be similar. Thus, we predict that our findings in rat models of neurotrauma can be used to help identify potential human therapeutic targets for brain trauma directed at COX-2 activation.

Objectives, year 5.

1-Simultaneous multiple analysis by *in vitro* transcription experiments to show levels of gene expression activation triggered by cryogenic injury.

2- Detection and quantification of cerebral infarction following ischemia- reperfusion using 2,3,5-Triphenyltetrazolium Chloride (TTC) stain (in rat and in mouse).

3- The effect of ischemia-reperfusion on COX-2 protein expression in rat brain and the effect of the PAF antagonist BN50730.

4- Middle cerebral occlusion in the mice: characterization of the model by cerebral blood flow measurements.

METHODS

Cryogenic Injury Protocol

The animal model of vasogenic brain injury is generated by the placement of a liquid nitrogen-cooled probe (b. P. -195.79°C) against the exposed skull of the rat during a one minute period. The cold probe consists of a brass rod 9 mm in diameter and 25 mm in length with a concave tip that fits against the curved surface of the skull. The probe is attached to a larger brass rod which acts as a heat sink 16mm in diameter and 55 mm in length. The rod is bound to a 30 cm stainless steel handle, the end of which is insulated with Delrin^R in order to prevent injuries to the operator during the experimental procedures. This probe is immersed in liquid nitrogen until the moment it is to be applied to the skull surface.

Albino Sprague Dawley rats weighing 150-220 gm are subjected to ether anesthesia. Their skulls are exposed by an incision along the scalp to the midline. The cold probe is then rapidly pressed onto the right fronto-parietal region of the skull for a period of one minute. The animals are sacrificed after injury at time points of one hour and one week. The control group undergoes the same procedure except for probe application. A rapid dissection on an ice-cold dissection board is performed, the right brain cortex is collected, and RNA is extracted. RNA extraction is performed according to a modification of Chomczynski and Sacchi method. The "in vitro" transcription technique applied during these studies allows the simultaneous detection of multiple genes in a single test. For detailed technical description see J. L. Cook et al. 1998 B.

Middle Cerebral Artery Occlusion

Focal cerebral ischemia is achieved in animals using the intraluminal technique developed by Zea Longa et al. Animals are fasted overnight. Anesthesia is induced with 3.5% halothane in a mixture of 70% nitrous oxide and 30% oxygen. Prior to intubation, animals are given an intraperitoneal injection of atropine sulfate (0.5mg/kg) in order to decrease salivation. Animals are orally intubated and mechanically ventilated during the procedure. During ventilation the animals are paralyzed with pancuronium bromide (dose 0.6mg/kg). After induction, halothane is reduced to 1% and adjusted thereafter according to blood pressure. An incision is made in the right groin and the proximal femoral artery and vein are isolated. Polyethylene catheters are placed in the vessels in order to measure arterial blood pressure and to deliver compounds. A vertical midline incision is made in the anterior neck and the common carotid artery is exposed. The external and internal carotid arteries are dissected from the bifurcation to the base of the skull. The branches of the external carotid artery are ligated. A small arteriotomy is made in the external carotid artery and the occluding nylon suture is introduced into the arterial lumen. The occluding suture is advanced into the internal carotid, and from there past the Circle of Willis, until it occludes the origin of the middle cerebral artery.

The suture is secured with a silk ligature. The neck incision is closed with 3-0 interrupted silk suture. The catheters in the groin vessels are capped, and the skin is closed with interrupted suture. Anesthesia is discontinued and the animals are extubated when awake. After two hours of ischemia, the animals are re-anesthetized with the above gas mixture delivered via the Fluovac anesthesia machine. Blood pressure is continuously monitored via the previously placed catheter. The neck incision is opened and the occluding suture is carefully removed from the arterial lumen, restoring blood flow to the territory of the middle cerebral artery. The catheters in the groin vessels are capped and the skin incisions closed with 3-0 silk suture. The animals are given oxygen as needed until they recover from anesthesia. The animals are returned to cages and given access to food and water.

Detection and Quantification of Cerebral Infarction

A reliable method for detecting and quantifying cerebral infarction in experimental animals is essential for the study of focal ischemia. 2,3,5-Triphenyltetrazolium Chloride (TTC) staining has been shown to be as effective as hematoxylin and eosin staining in revealing the extent of infarction in cerebral tissue (Bederson et al., 1986a; 1986b). Anesthesia is induced with 3.5% halothane in a mixture of 70% nitrous oxide and 30% oxygen. After the animal is anesthetized, it is removed from the induction chamber and immediately decapitated. The brain is carefully removed and placed in ice cold saline. The chilled brain is embedded in 3% agar gel and mounted on a plastic stage. Using the Rotorslicer, the brain is cut into several one millimeter thick coronal slices. These slices are carefully transferred to dishes that contain a 2% solution of TTC in saline at 37°C. Slices are immersed in this solution for thirty minutes, after which the TTC solution is replaced with 10% phosphate buffered formalin. The staining process produces a brick red color in viable tissue and leaves injured tissue unstained. Using a digital camera, images of the slices are captured and stored for analysis.

Measurement of Cerebral Blood Flow

Variability of the size and location of infarcts between experimental animals is one of the problems we have encountered with this model of focal ischemia. Subtle differences of cerebrovascular architecture between animals and difficulty placing the occluding suture in the correct position are probably to blame for much of the variability between animals. A reliable method for calculating cerebral blood flow allows us to group animals that have experienced a similar degree of ischemia. Anesthesia is induced with 3.5% halothane in a mixture of 70% nitrous oxide and 30% oxygen. After induction, halothane is reduced to 1% and delivered via the Fluovac anesthesia machine. The skin incision in the groin is opened and the femoral artery and vein catheters are inspected for patentcy. Four μCi of iodo[^{14}C]antipyrine (approximately

100µl) are pumped into the vein catheter at a constant rate. Blood is simultaneously withdrawn through the arterial catheter. After forty-five seconds, the catheters are clamped and the animal is decapitated. The brain is carefully removed and placed in liquid nitrogen. The radioactive animal carcass is properly disposed of. The brain is sliced into twenty-micron thick slices using a cryostat. Each of five slices is saved, placed in a cover slip and left to dry on a slide warmer until tissue is well dry. Cover slips are then arranged on a board, together with a ^{14}C-plastic standard range and installed into an autoradiographic exposure envelope with a phosphor plate or X ray film. After a period of 3 days, the phosphor plate samples are scanned with a Fuji phosphoimager; after 10 days the X ray film samples are developed. After data capture of autoradiographic images, analysis of cerebral blood flow is obtained by use of an image alignment algorithm (Zhao et al., 1993) based on the original equation described by Kety (1996):

$$Ci(T)=\lambda K\int_o^t C_A e^{-K(T-t)}dt$$

Ci(T)= tissue concentration of ^{14}C Iodo Antipirin at time T
λ= tissue:blood partition coefficient,
C_A= concentration of tracer in arteril blood
t= variable time
K= mf/wλ = the rate of blood flow
m= a constant between 0 to 1 which represents defusion equilibrium of the radiolabeled compound between blood and tissue

Simultaneous analysis of multiple gene expression by *in vitro* transcription.

Brain tissue is rapidly dissected on an ice cold dissection board, and brain cortex rapidly removed. Total RNA from brain regions is isolated following the guanidinium-thiocyanate-phenol-chloroform method of Chomczynski and Sacchi (1987). Tissue is homogenized with a Polytron type homogenizer, in 4 ml buffer containing 4 M Guanidine Thiocyanate, 25 mM sodium citrate, 0.5 % n-lauroyl sarcosine, and 0.1 M mercaptoethanol, pH 7.0. After precipitation, the newly purified RNA extract is resuspended in DEPC (diethyl-pirocarbonate) treated water, and an aliquot is quantified by spectrophotometric detection in a range of 300 to 220 nm. The sample RNA is divided in 50 µg aliquots, then ethanol precipitated and stored at -80 °C until ready to start the *in vitro* transcription assay. *In vitro* transcription assay is performed as follows: Sample RNA after precipitation is re-suspended in 50 µl of DEPC-water, then 40 µl of Master Mix-1 [per sample contains: 20 µl 5x fist strand buffer, 10 µl 0.1 M DTT, 5 µl dNTPs,

and 5 µl (^{32}P)dCTP]. The sample is then pre incubated at 37 °C for two min, then add 10 µl of reverse transcriptase (200 µg/µl) added and incubated for 2 hours at 37 °C. The reaction is terminated by placing on ice, adding 2 µl random primers (pdN_6 5 µg/µl), and placing in 90 °C water bath for 10 min, then on ice for 5 min. 35 µl of Master Mix-2: [5 µl 0.5 mM dNTPs (without dCTP), 15µl of 10x klenow buffer, and 10 µl (^{32}P)dCTP and 5 µl klenow (1 µg/µl)]are then added to each sample and incubated at 37 °C overnight. Volumes are normalized to 200 µl with TE pH 8 buffer and centrifuged through Bio-Spin 30 columns. Eluates are loaded into hybridizations bags with nitrocelulose membranes containing Dot-Blots of all the cDNA probes intended for study (5 µg per dot) and incubated for 24 hours at 42 °C. Finally, membranes are washed twice at room temperature in 0.1xSSC, 0.1% SDS for 15 min. The procedure is repeated at 50 °C. Membranes are then exposed to x-ray film or phosphoimager plate for identification and quantitative analysis purposes. For more detailed technical description refer to J. L. Cook et al. 1998 B.

Protocol for COX-2 Western-blotting rat brain tissues.

Tissue samples are kept in ice until homogenization. Hippocampal tissue is then rapidly homogenized in a 2 ml glass/glass homogenizer with 0.5 ml of lysis buffer (10 mM Tris-HCl, 10 mM EDTA, 5mM EGTA, 1 % Triton-X-100, pH 7.4. Protease inhibitors are added just before use: 0.1M PMSF, 0.1TIU/ml Aprotinin, and 0.1M Leupeptin) at room temperature. Homogenates are sonicated for 30 seconds. The concentration of protein of the samples is measured, and lysis buffer used as alicuots on standard curve and blanks to correct for protease inhibitors. Proteins are diluted to a concentration of 10 µg proteins in 10 µl lysis buffer. Equal volumes of 2 X concentrated electrophoresis sample buffer(250 mM Tris-HCl, pH 6.5, 2 % SDS, 10 % glycerol, 0.006 % Bromophenol Blue, and 10 µl/ml Mercaptoethanol) are added to each sample. Samples are kept on ice and boiled for 3 - 5 min. just before gel loading. The electrophoresis apparatus preparations and gel casting are started before tissue homogenization. Samples (20 µl per well) are loaded onto a 0.75 - 1.00 mm thick SDS-polyacrylamide gel and run at 180 to 200 volts for about 45 to 60 min. For gel transfer, the gel is soaked in ice cold transfer buffer (4°C) for 30 min to allow the gel to shrink to final size. Residuals of running buffer can then be removed. Gel and nylon membrane are installed on transfer apparatus; transfer is initiated at 100 V for about 1 hour. The apparatus is then dissassembled, the membranes removed from the cassettes by help of a soft pencil, the position of main bands marked, and the side where the proteins are bound labeled. The membranes are soaked in blocking buffer overnight at 4 °C, or for 30 min at 37 °C on an oscillatory platform, then incubated at 37 °C with the primary antibody for 30 min. The primary antibody is diluted in 10 ml of blocking buffer. Antibody dilutions are: PGHS-1 1/2000 (Polyclonal Anti-PGHS-1) Cat.# M-20 Santa Cruz. PGHS-2 1/2000 (Monoclonal Anti-PGHS-2)

Cat.# 16011 Cayman. The membranes are washed in fresh blocking buffer, then placed in weighing buckets with 25 ml blocking buffer at room temperature on a rocking platform. The buffer is replaced every 5 min until completed at 30 min. Membranes are incubated at 37 °C with secondary antibody for 30 min in the rotatory oven. The secondary antibody is diluted in 10 ml of blocking buffer, Anti-Mouse IgG 1/2000 (Anti-Mouse IgG horseradish peroxidase conjugate) Catalog # M15345L3. Transduction Laboratories.

For Alkaline phosphatase, 1/10,000 dilution of secondary antibody is used. The membranes are washed in the blocking buffer and placed in weighing buckets with 25 ml blocking buffer at room temperature on a rocking platform. The buffer is replaced every 5 min for 30 minutes.

RESULTS.

1-Simultaneous analysis of several gene expression triggered by cryogenic injury.

To test the linearity of a quantitative analysis by use of this novel technique, increasing amounts of p53 RNA were added to a control RNA extract from rat brain tissues. Control RNA aliquots received 0, 0.5, 1, 2, 4, and 8 ng of p53 RNA . *In vitro* transcription was performed on those samples, then hybridized to nitrocellulose membranes which previously were loaded with 5 µg each of plasmid cDNAs. The cDNA chosen were: p53, IGF-1, Transferrin receptor, and bFGF. **Figure 1** shows that, as expected, increasing amounts of p53 RNA produced a proportional response on the membranes; meanwhile no changes were observed for the other genes after quantitative analysis. Data plot for p53 is shown in **figure 2**, in which a linear response was detected. To compare the relative expression levels of different genes in controls one hour or one week after cryogenic injury, samples obtained from rat brain cortex treated accordingly were hybridized with membranes containing multiple cDNAs. Two cDNA controls were obtained by loading just the plasmid cDNA, without insert (pUC19 and pBR322 were the plasmids used for this purpose). Then somatostatin, myelin basic protein (MBP), proteolipid protein (PLP), glial fibrillary acidic protein (GFAP), thymidine kinase (TK), insulin-like growth factor-1 (IGF-1), renin, and c-fos were also loaded. In **figure 3**, the different profiles obtained are shown. As expected, typical early gene response was shown for c-fos, which rises rapidly at 1 hour and completely returns to normal by 1 week. The other studied genes showed altered profiles, which became significative by 1 week. Although already elevated after 1 hour and 1 week, thimidine kinase and renin showed a different pattern with a smaller increase.

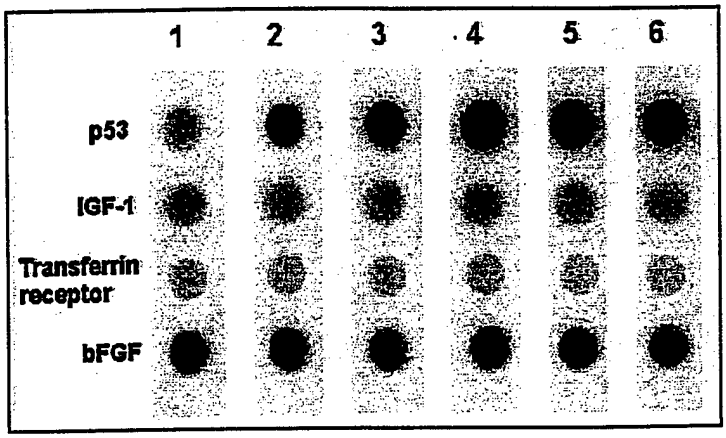

Figure 1. P53 *in vitro* transcribed RNA (0.5, 1, 2, 4, and 8 ng) was added to a 0 h cerebral RNA and resulting radiolabeled cDNA products were hybridized to nitrocellulose filter-fixed clones.

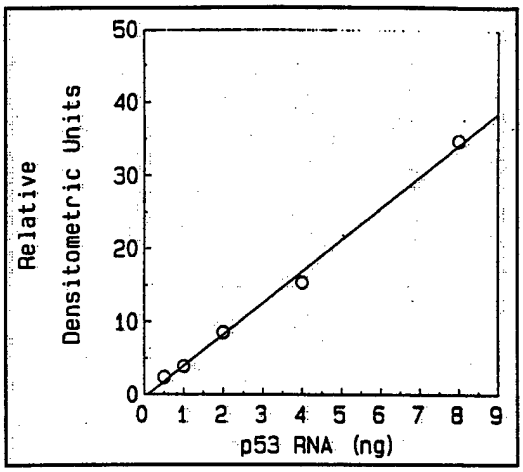

Figure 2. Densitometric evaluation of p53 signals presented in Fig. 1.

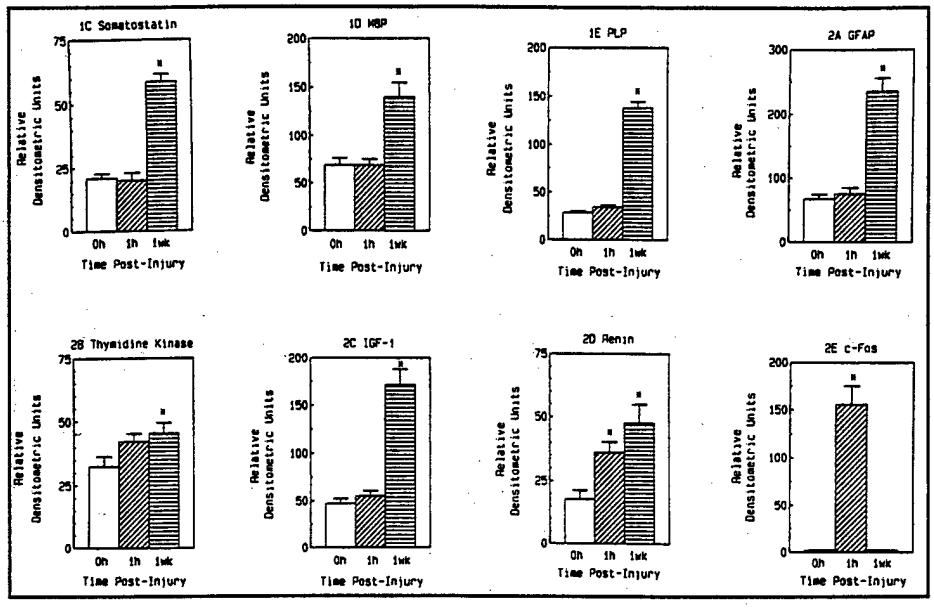

Figure 3. Graphical illustrations of cortex-derived radiolabeled cDNAs bound to filter-fixed clones, as a function of time post-injury. Bars represent mean ±SD of three unrelated experiments. Asterisk denotes value significantly greater than 0 h control ($p<0.05$).

2- Detection and quantification of cerebral infarction following ischemia- reperfusion using 2,3,5-Triphenyltetrazolium Chloride (TTC).

In order to determine the reproducibility of the animal model, we evaluated the infarcted area by use of the 2,3,5-Tryphenyltetrazolium Chloride (TTC) staining technique after middle cerebral artery occlusion and reperfusion. Both the rat and mouse animals models were studied with this histochemical technique. In normal tissues the TTC salts are reduced by dehydrogenases, changing to a red brick color of the tissues. When dehydrogenase activity drops as result of ischemic damage no change of color occurs, so tissue remains unstained. In **figure 4** is shown a typical staining obtained in a rat after 2 hours of middle cerebral artery occlusion and 5 days of reperfusion. The animal brains were cut coronally in 10 sections of equal thickness. A diagram for rats and mice is shown in **figure 6**. After staining, images were captured with a digital camera mounted to a dissection microscope. A similar pattern of staining was obtained from mice brain tissues as shown in **figure 5**, were a well defined infarcted area is found on the cortical region of most of the slices studied. The infarcted areas were calculated as percentile of the total area in the slice and average profiles are shown in **figure 7** for rat and mice (Bederson et al., 1986b). It is important to note that a consistent neurological score of 2 (0: no deficit, 1: flexion of contralateral fore paw, 2: circling, 3: spining, leaning or no spontaneous movement) was obtained for all the animals taken into consideration for this study. This study was followed by the analysis of the cerebral blood flow shown below in section 4.

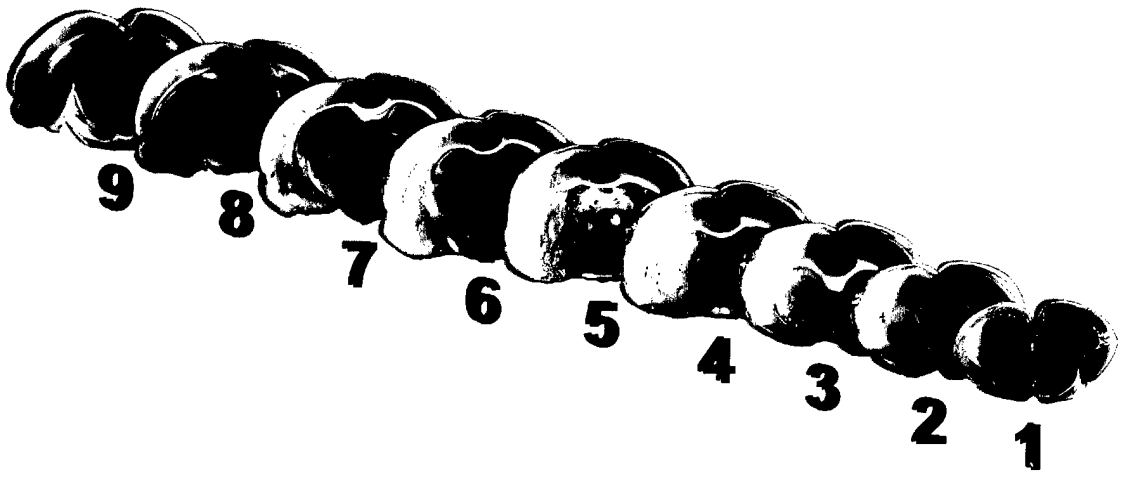

Figure 4. Images of rat brain slices stained with TTC to determine the focal area of damage after ischemia-reperfusion. After 2 hour MCO and 5 days of reperfusion, animals were killed, brain tissue removed at 4°C and rapidly sliced in 1 mm thick sections. Sections were immersed in 2% TTC stain for 30 min. Tissue images were captured with a digital camera mounted in a dissection microscope. Here is shown a composition of a representative rat brain.

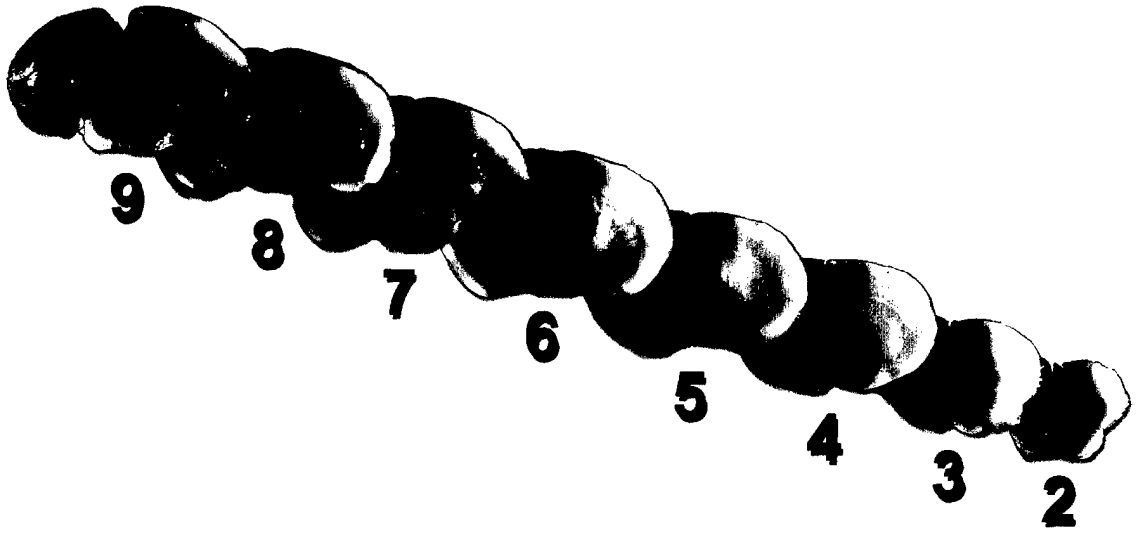

Figure 5. Images of mouse brain slices stained with TTC to determine the focal area of damage after ischemia-reperfusion. Details as in Figure 4 legend.

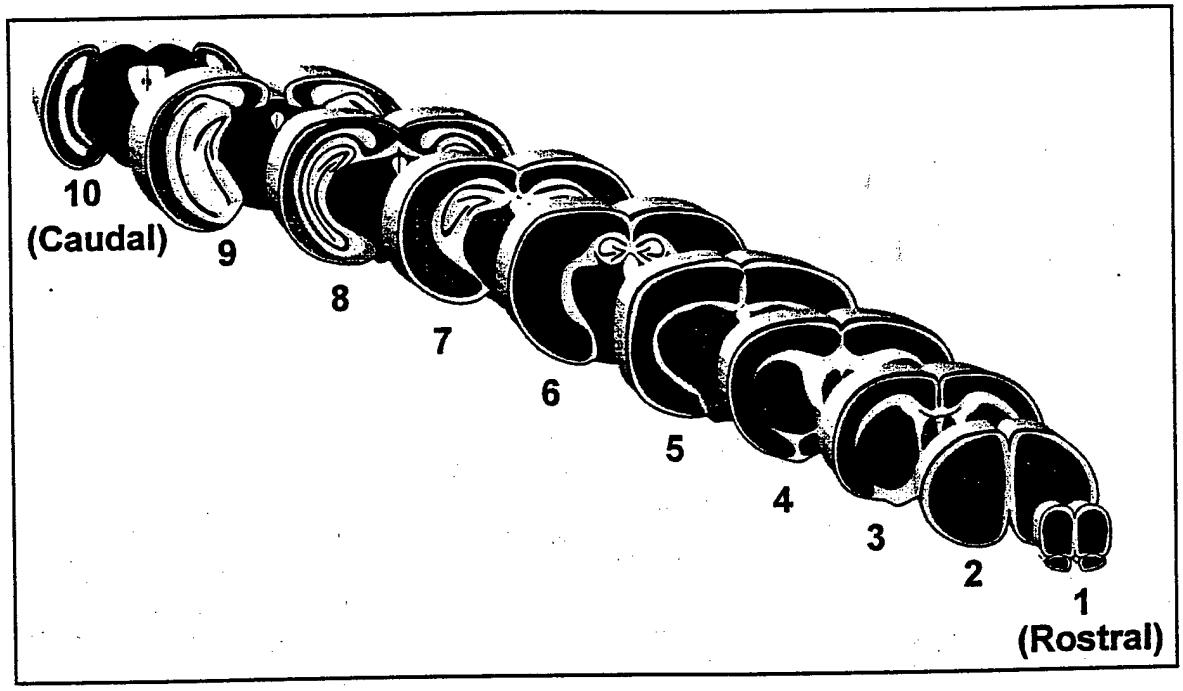

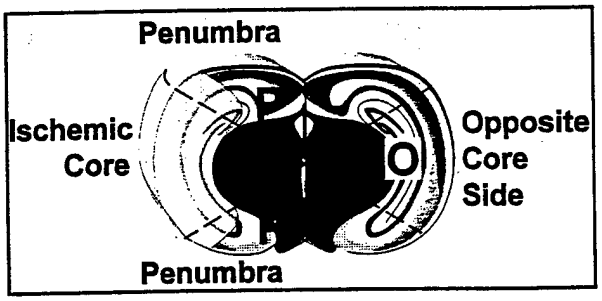

Figure 6. Diagram of focal ischemia after middle cerebral artery occlusion in the rat brain. This diagram shows the procedure of slicing and collection of tissue for Western blot analysis. Slices 1, 2, 3, 6, 9 and 10 were stained with TTC to be able to determine the position of infarcted area.

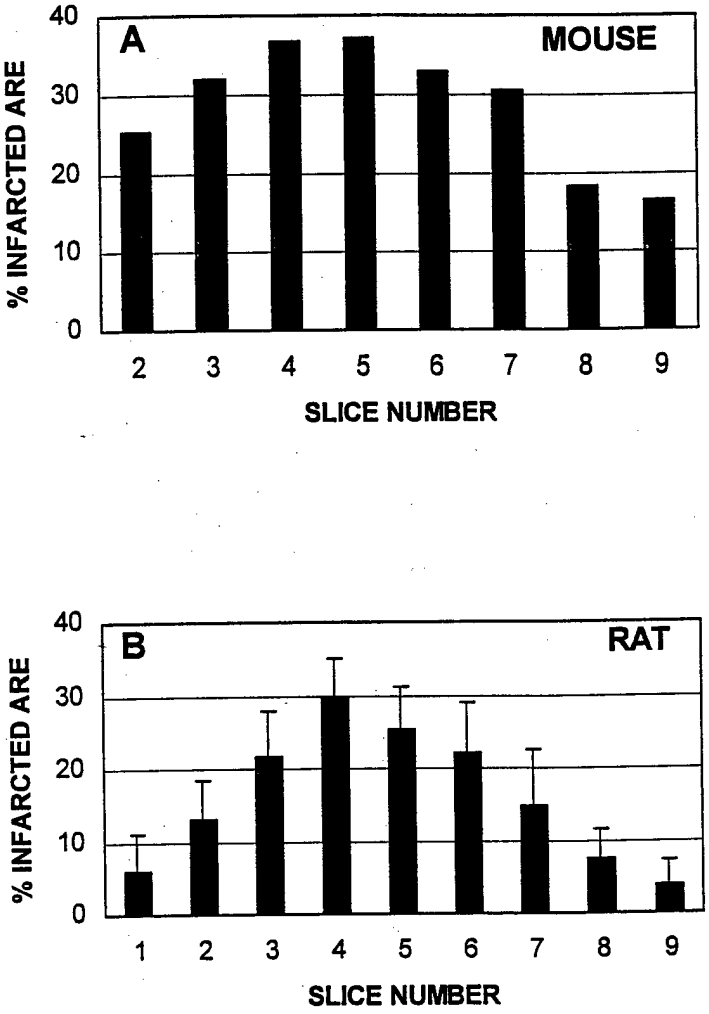

Figure 7. Percent area infarcted to total slice area of the mouse and rat brain after ischemia-reperfusion. A)shows data obtained for a representative mouse after 2 hour MCO and 5 days reperfusion. Values were obtained from images shown in Figure 6. B) mean values ±SD (n=12 rats) are shown. A representative image series is shown in Figure 5.

3- The effect of ischemia-reperfusion on COX-2 protein expression in rat brain and the effect of the PAF antagonist BN50730.

Brain damage triggered by ischemia-reperfusion, is initiated by an inflammatory cascade which involves activation of PLA_2 and the release of injury mediators, including free AA and PAF. Because PAF is a transcriptional activator of COX-2, via its interaction with an intracellular receptor selectively blocked by the antagonist BN50730, we evaluate the expression of COX-2 protein and the effect of BN50730 following two hours of ischemia and three hours reperfusion. Focal ischemia in the right temporal cortex was induced by middle cerebral artery occlusion and BN50730, when present, was administered by intracerebroventricular injection at the onset of the ischemic episode. Ischemic core and penumbra areas were dissected following 3 hours reperfusion. Contralateral brain (left cortex) was used as a control. Proteins were extracted and COX-2 protein determined by Western blot.

In the ischemic core, COX-2 expression was increase by 220% as compared to control and in the penumbra the increase was even higher (239%) (**Figure 8**). In BN50730 treated animals values attained in the core and penumbra were 141% and 104%, respectively. Thus, BN50730 treatment inhibited COX-2 expression in the core by 36% as compared to untreated animals. In the penumbra, the expression induced by ischemia-reperfusion was inhibited by 100%.

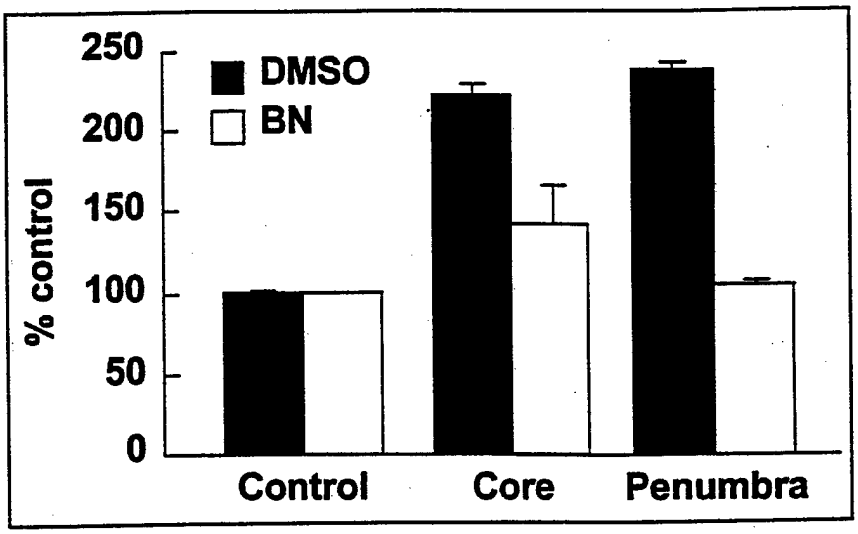

Figure 8. Brain COX-2 protein levels in a rat model of focal ischemia-reperfusion. After 2 hours ischemia followed by 3 hours reperfusion, the core and penumbra areas were dissected, proteins extracted and COX-2 protein quantified by Western blot. BN50730 (15 µg/2µl DMSO) was administered intracerebroventricularly (in the right and left ventricles) before artery occlusion. Control samples were taken from the contralateral cortex. Mean values ± SD from n=3 individual samples are shown.

4- ***Middle cerebral artery occlusion in the mice: characterization of the model by cerebral blood flow measurements.***

To further assess the reproducibility of this method in our laboratory for its use on mice, a technique for cerebral blood flow measurement at the time of occlusion and at 2 hours of reperfusion was developed. We modified a technique devised in rats (W. Zhao et al., 1993) and applied it for the mouse. The results, although preliminary, show a reproducible pattern. In **figure 9 A** is shown a typical autoradiographic display of the blood flow where the use of a grey scale was applied to facilitate the appreciation of small differences in radioactivity levels. Black represents high levels of radioactivity, and white represents no radioactivity (no blood flow). As shown in **figure 9 A**, a typical drop in blood flow appears in the right lower section of the cortical brain which correlates with the infarcted area shown on figure 5 obtained with TTC stain. When animals after the ischemic insult were left to reperfuse for two hours, by removal of intraluminal suture, blood flow was almost completely restored, see **figure 9 B** only a faint shadow appears in a typical analysis. This indicates that blood flow has been restored as expected, and the ischemic infarction was caused by the damage generated during occlusion only. The quantitative analysis by computer integration of autoradiographic images are underway.

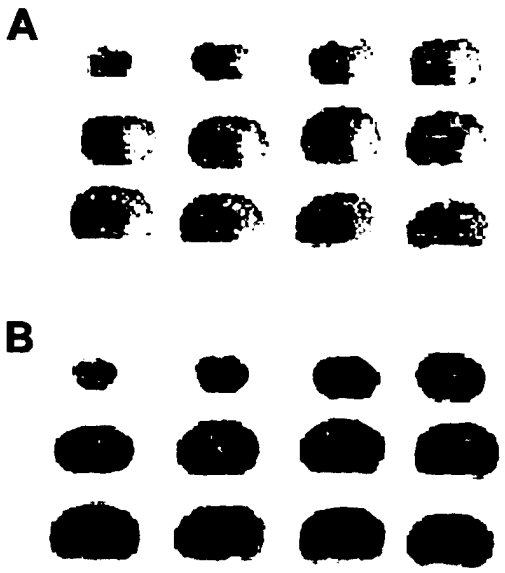

Figure 9. Autoradiographic measurements of cerebral blood flow by the Iodo-[^{14}C] antipyrine method in the mouse brain. (a) mouse brain 2 hours of MCA occlusion; (b) mouse brain after 2 hours of MCA occlusion and 2 hours reperfusion. Larger accumulation of radioactive marker occurs with faster cerebral blood flow; pale or clear areas indicate low cerebral blood flow.

7- SUMMARY AND CONCLUSIONS

1- a) A novel technical approach was developed to rapidly and simultaneously detect expression levels of different genes in very small tissue samples. b) By use of this technique in cryogenic injured animals it is possible to evidence differential profiles of gene expression, as those obtained for early genes (c-fos), intermediate genes (thimidine kinase, renine), and genes which show over-expression only after 1 week (somatostatin, myelin basic protein, proteolipid protein, glial fibrillary acidic protein, insulin-like growth factor-1).

2- a) Using TTC staining we have shown that middle cerebral occlusion in both rats and mice, results in a well defined focal ischemic area that accounts for up to 40% of total slice area.
b) both mice and rats showed consistent results with this technique, which indicates the applicability of this animal model for studies on rat transgenic animals and mouse knock-outs.

3- Ischemia-reperfusion induces COX-2 expression both in the core and in the penumbra areas of the focal ischemic insult. Interestingly, BN50730 inhibited COX-2 expression in both areas but to a greater extent in the penumbra area. This observation is highly relevant, indicating that neurons damaged in this area can be protected from COX-2 signaling pathway leading to free radicals production and prostaglandin synthesis.

4- Cerebral blood flow analysis in mouse brain after ischemia-reperfusion indicates:
a) a well defined and reproducible focal ischemic area after 2 hours middle cerebral artery occlusion.
b) recovery of brain circulation at the end of 2 hour recirculation, which is an important observation to demonstrate that animals were following an almost complete reperfusion condition. Removal of the intra luminal suture does not produce further alterations other than that generated by the post-ischemic edema which, as expected, produces a small decrease in cerebral blood flow.

8- REFERENCES

Bazan, N. G., Squinto, S. P., Braquet, P., Panetta, T., and Marcheselli, V. L. (1991). Platelet-activating factor and polyunsaturated fatty acids in cerebral ischemia or convulsions: intracellular PAF-binding sites and activation of a Fos/Jun/AP-1 transcriptional signaling system. Lipids 26: 1236-1242.

Bazan NG, Allan G, Rodriguez de Turco EB (1993). Role of phospholipase A_2 and membrane-derived lipid second messengers in excitable membrane function and transcriptional activation of genes: Implications in cerebral ischemia and neuronal excitability. Prog in Brain Res 96:247-257.

Bazan, N. G. (1994). Signals, messengers and genes in cerebral ischemia: Novel sites for neuroprotection . In: Krieglstein, J. and Oberpichler, -Swenk, H (eds) Pharmachology of cerebral ischemia, pp. 1-13. Stuttgart: Wissenschaftl.

Bazan NG, Fletcher BS, Herschman HR, Mukherjee PK. (1994.) Platelet-activating factor and retinoic acid synergistically activate the inducible prostaglandin synthase gene. Proc. Nat. Acad. Sci. USA. 91:

Bazan NG, Rodriguez de Turco EB, Allan G (1995): Mediators of injury in neurotrauma: Intracellular signal transduction and gene expression. J Neurotrauma 12(5):791-814, 1995.

Bazan NG: (1995) Inflammation: A signal terminator. Nature 374:501-502.

Baba, T., Black, K. L., Ikezaki, K., Chen, K., and Becker, D. P. (1991). Intracarotid infusion of leukotriene C_4 selectively increases blood-brain-barrier permeability after focal ischemia in rats. J. Cer. Blood Flow Metab. 11, 638-643.

Bederson, J. B., Pitts, L. H., and Tsuji, M. (1986a). Rat middle cerebral artery occlusion: Evaluation of the model and development of a neurologic examination. Stroke 17, 472-476.

Bederson, J. B., Pitts, L. H., Germano, S. M., Nishimura, M. C., Davis, R. L. And Bartkowski, H. M. (1986b). Evaluation of 2, 3, 5-triphenyltetrazxolium chloride as a stain for detection and quantification of experimental cerebral infarction in rats. Stroke 17, 1304-1308.

Benveniste, H., Drejer, J., Schousboe, A., and Diemer, N.H. (1984). Elevation of the extracellular concentrations of glutamate and asparate in rat hippocampus during trancient

cerebral ischemia monitored by intracerebral microdialysis. J. Neurochem. 43, 1363-1374

Bonventre, J.V., Huang, Z., Taheri, M.R., O'Leary, E., Li, E., Moskowitz, M.A., Sapirstein, A. (1997) Reduced fertility and postischaemic brain injury in mice deficient in cytosolic phospholipase A_2. *Nature* 390: 622.

Braquet et al., 1987.

Choi, D.W. (1988). Glutamate neurotoxicity and diseases of the Nervous system. Neuron 1, 623-534.

Christensen, T., Bruhm, T., Diemer, N.H., and Schousboe, A. (1991). Effect of phenylsuccinate on potassium- and ischemia-induced release of glutamate in rat hippocampus monitored by microdialysis. Neuroscience Letter 134,71-74.

Clark, G. D., Happel, L. T., Zorumski, C. F., and Bazan, N. G. (1992). Enhancement of hippocampal excitatory synaptic transmission by platelet-activating factor. Neuron 9: 1211-1216.

Collaco-Moraes Y, Aspey B, Harrison M, de Belleroche J. 1996. Cyclo-oxygenase-2 messenger RNA induction in focal cerebral ischemia. J. Cereb. Blood Flow Metab. 16:1366-1372.

Cook, J. L., Marcheselli, V., Alam, J., Deininger, P. L. and Bazan, N. G. (1998). Temporal changes in gene expression following cryogenic rat brain injury. Mol. Brain Res. 55:9-19.

Cook, J. L., Marcheselli, V., Alam, J., Deininger, P. L. and Bazan, N. G. (1998). Simultaneous analysis of multiple gene expression patterns as a function of development, injury or senescence. Brain Res. Prot. 3, 1-6.

Faden, A.I., Demediuk, P., Panter, S.S., and Vik, R. (1989).The role of excitatory amino acids and NMDA receptors in traumatic brain injury. Science 244, 798-800.

Farooqui AA. Yang HC. Horrocks L. (1997). Involvement of phospholipase A2 in neurodegeneration. Neurochem Internat. 30:517-22.

Herschman, H. R. (1994). Regulation of prostaglandin synthase-1 and prostaglandin synthase-2. Cancer and Metastasis Rev. 13:241-256.

Herschman H.R. (1996). Prostaglandin synthase 2. Biochim Biophys Acta. 1299:125-40.

Katayama, Y., Becker, D. P., Tamura, T., and Hovda, D. A. (1990). Massive increase in extracellular potassium and the indiscriminate release of glutamate following concussive brain injury. J. Neurosurg. 73: 889-900.

Kaufmann, W.E., Worley, P.F., Pegg, P.J., Bremer, M., and Isakson, P. (1996) COX-2, a synaptically induced enzyme, is expressed by excitatory neurons at postsynaptic sites in rat cerebral cortex. *Proc. Natl. Acad. Sci.* 93:2317-2321.

Kety, S. S. (1960). Measurement of local blood flow by the exchange of an inert, diffusible substance. Methods Med. Res. 8, 228-236.

Marcheselli, V. L., Rossowska, M., Domingo, M. T., Braquet, P., and Bazan, N. G. (1990). Distinct platelet-activating factor binding sites in synaptic endings and in intracellular membranes of rat cerebral cortex. J. Biol. Chem. 265, 9140-9145.

Marcheselli, V. L. And Bazan, N. G. (1994). Platelet-activating factor is a messenger in the electroconvulsive shock-induced transcriptional activation of c-fos and zif-268 in hippocampus. J. Of Neurosci. Res. 37: 54-61.

Mitani, A., Imon, H., Iga, K., Kubo, H., and Kataoka, K. (1990). Gerbil hippocampal extracellular glutamate and neuronal activity after trancient ischemia. Brain Res. Bull 25, 319-324.

Moncada, S., and Vane, J. P. (1979). Pharmacology and endogenous roles of prostaglandin endoperoxides, thromboxane A_2 and prostacyclin. In: Munson, P. L. (Ed) Pharmachology Review, pp 293-331. Baltimore: Williams and Wilkins.

Nilsson, P., Hillered, L., Pontn, U., and Ungerstedt, U. (1990). Changes in cortical extracellular level of energy-related metabolites and amino acids following concussive brain injury in rats. J. Cereb. Blood Flow Metab. 10, 631-637.

Nogawa S, Zhang F, Ross ME, Iadecola C. 1997. Cyclo-oxygenase-2 gene expression in neurons contributes to ischemic brain damage. J. Neurosci. 17: 2746-2755.

Olney. J. W. (1986). Inciting excitotoxic cytocide among central neurons. Adv. Exp. Med. Biol. 203, 631-645.

Panetta T, Marcheselli VL, Braquet P, Spinnewyn B, Bazan NG. (1987) Effects of a platelet-activating factor antagonist (BN 52021) on free fatty acids, diacylglycerols, polyphosphoinositides and blood flow in the gerbil brain: Inhibition of ischemia-reperfusion induced cerebral injury. Biochem Biophys Res Commun. 149:580-587.

Piomelli, D. (1994). Eicosanoids in synaptic transmission. Critical Rev. in Neuribiol. 8, 65-83.

Planas AM, Soriano MA, Rodriguez-Farre E, Ferrer I. 1995. Induction of cyclooxygenase-2 mRNA and protein following transient focal ischemia in the rat brain. Neurosci. Lett. 200: 187-190.

Rothman, S.M., and Olney, J.W. (1986). Glutamate and the pathophysiology of hiposic-ischemic brain damage. Ann. Neurol. 19, 105-111.

Shimizu, T., and Wolfe, L. S. (1990). Arachidonic acid cascade and signal transduction. J. Neurochem. 55, 1-15.

Squinto SP, Block AL, Braquet P, Bazan NG (1989) Platelet-activating factor stimulates a Fos/Jun/AP-1 transcriptional signaling system in human neuroblastoma cells. J Neurosci Res 24:558-566.

Unterberg, A., Wahl, M., Hammerson, F., and Baethman, A. (1987). Permeability and vasomotor response of cerebral vessels during exposure to arachidonic acids. Acta Neuropathol. (Berl.) 73, 209-211.

Volterra, A., Trotti, D., Cassuti, P., Tromba, C., Galimberti, R., Lecchi, P.,and Ragani, G. (1992). A role for the arachidonic acid cascade in fast synaptic modulation: ion channels and transmitter uptake systems as target proteins. Adv. Exp. Med. Biol. 318, 147-158.

Yamagata K, Andreasson KI, Kaufmann WE, Barnes CA, Worley PF. (1993). Expression of a mitogen-inducible cyclooxygenase in brain neurons: regulation by synaptic activity and glucocorticoids. Neuron 11: 371-386.

Zhao, W., Young, T. Y., and Ginsberg, M. D. (1993). Registration and three-dimensional reconstruction of autoradiographic images by the disparity analysis method. IEEE Trans Med. Imag. 12, 782-791.

Reprinted from

BRAIN RESEARCH PROTOCOLS

Brain Research Protocols 3 (1998) 1–6

Protocol

Simultaneous analysis of multiple gene expression patterns as a function of development, injury or senescence

Julia L. Cook [a,b,c,*], Victor Marcheselli [b], Jawed Alam [a,c], Prescott L. Deininger [a,c], Nicolas G. Bazan [b]

[a] *Ochsner Medical Foundation, Division of Research, New Orleans, LA, USA*
[b] *Ophthalmology and Neuroscience Center, LSUMC, New Orleans, LA, USA*
[c] *Biochemistry and Molecular Biology, LSUMC, New Orleans, LA, USA*

ELSEVIER

BRAIN RESEARCH PROTOCOLS

SCOPE AND PURPOSE

BRAIN RESEARCH PROTOCOLS will publish current and updated protocols in neuromorphology, cellular and molecular neurobiology, neurophysiology, developmental neurobiology, neuropharmacology, quantitative and computational neurobiology, and behavioral neurobiology. The overriding criteria for publication are significant methodological and experimental relevance to a multidisciplinary audience.

TYPES OF PAPERS

1. **Protocols:** complete, full-length protocols.

2. **Protocol Updates:** updates on published protocols submitted by the author thereof, describing new developments which are of sufficient interest to the neuroscience community, but which do not warrant a completely new submission. The maximum length allowed will be 1500 words or equivalent space in tables and illustrations.

3. **Technical Tips:** comments on published protocols describing useful hints and "tricks" related to any aspect of the protocol, such as timing, equipment, chemicals, troubleshooting, etc., to be published at the discretion of the Editor within a newsgroup-style forum on the WWW linked to the on-line version of the journal.

SUBMISSION OF MANUSCRIPTS

Submission of a paper to ***Brain Research Protocols*** is understood to imply that it deals with original material not previously published (except in abstract form), and that it is not being considered for publication elsewhere. Manuscripts submitted under multiple authorship are reviewed on the assumption that all listed authors concur with the submission and that a copy of the final manuscript has been approved by all authors and tacitly or explicity by the responsible authorities in the laboratories where the work was carried out. If accepted, the article shall not be published elsewhere in the same form, in either the same or another language, without the consent of the Editors and Publisher. The Publisher and Editor regret that they are unable to return copies of submitted articles except in the case of rejected articles, where only one set of manuscript plus figures will be returned to the author.

Manuscripts in English should be organised according to the *Guidelines for the Submission of Manuscripts* and sent *in triplicate* (including three copies of all illustrations) to the Editor:

Dr. Floris G. Wouterlood, Department of Anatomy, Faculty of Medicine, Free University, van der Boechorststraat 7, 1081 BT Amsterdam, The Netherlands; Fax: (31) (20) 444-8054; E-mail: fg.wouterlood.anat@med.vu.nl

Correspondence regarding accepted manuscripts relating to proofs, publication and reprints should be sent to:
Brain Research, Elsevier Science B.V., P.O. Box 2759, 1000 CT Amsterdam, The Netherlands. Tel. (31) (20) 485-3435; Fax: (31) (20) 485-3271; E-mail: g.house@elsevier.nl

EDITORIAL BOARD

GUIDELINES FOR THE SUBMISSION OF MANUSCRIPTS

These can be found on the **Brain Research Interactive** Website (**http://www.elsevier.com/locate/bres** or **http://www.elsevier.nl/locate/bres**) as well as in the "front matter" of every issue of the journal.
The preferred medium of submission is on disk with accompanying manuscript (see "Electronic manuscripts").

ELSEVIER

Brain Research Protocols 3 (1998) 1–6

BRAIN RESEARCH PROTOCOLS

Protocol

Simultaneous analysis of multiple gene expression patterns as a function of development, injury or senescence

Julia L. Cook [a,b,c,*], Victor Marcheselli [b], Jawed Alam [a,c], Prescott L. Deininger [a,c], Nicolas G. Bazan [b]

[a] *Ochsner Medical Foundation, Division of Research, New Orleans, LA, USA*
[b] *Ophthalmology and Neuroscience Center, LSUMC, New Orleans, LA, USA*
[c] *Biochemistry and Molecular Biology, LSUMC, New Orleans, LA, USA*

Accepted 11 March 1998

Abstract

Concurrent changes in expression of eight genes were examined following cryogenic rat brain injury. Cortical RNA levels were catalogued at time 0, and at 1 h and 1 week following injury. The genes include thymidine kinase (TK), c-*fos*, renin, myelin basic protein (MBP), proteolipid protein (PLP), glial fibrillary acidic protein (GFAP), insulin-like growth factor-1 (IGF-1), and somatostatin. All demonstrate increased expression following injury. Renin and c-*fos* exhibit detectable changes as early as 1 h post-injury.

Themes: Cell biology

Topics: Gene structure and function: general

Keywords: Injury; Cryogenic; Growth factor

1. Type of research

The described protocol is appropriate for:

- simultaneous quantification of tens to hundreds of low copy number messages.
- Studies of regulation of gene expression following injury, drug administration, or genetic alteration, and during normal development, differentiation, and senescence.

2. Time required

- RNA extraction: 2 h.
- First strand cDNA synthesis and analysis of product: 3 h.
- Second strand cDNA synthesis and radiolabeled probe preparation: 1 h (hands-on), overnight incubation.
- Preparation of filter-fixed plasmid probes, prehybridization: 2 h (hands-on), 5 h incubation, overnight incubation.
- Hybridization: 24 h or more.
- Film exposure: 48–72 h.

3. Materials

3.1. Chemicals and reagents

Guanidine thiocyanate salt, isoamyl alcohol, sodium acetate, glycine, salmon sperm DNA, ficoll, polyvinylpyrrolidone and diethyl pyrocarbonate (DEPC) were from Sigma (St. Louis, MO, USA). Phenol was from United States Biochemical (Cleveland, OH, USA). Mallinckrodt brands of chloroform, formamide and sodium phosphate were from Baxter/Scientific Products (McGaw Park, IL, USA). Ethanol was from Pharmco (Brookfield, CT, USA). M-MLV, Oligo $(dT)_{12-18}$, 5 × First Strand Buffer, 1 kb DNA ladder (1 $\mu g/\mu l$) and 0.1 M dithiothreitol (DTT) were from Gibco/BRL (Gaithersburg, MD,

* Corresponding author. Ochsner Medical Foundation, Division of Research, New Orleans, LA, USA. Fax: +1-504-842-3381; E-mail: jcook@ochsner.org

1385-299X/98/$ - see front matter
PII: S1385-299X(98)00012-9

USA). [α-^{32}P]dCTP (3000 Ci/mmol) was from Dupont NEN (Boston, MA, USA). Deoxyribonucleotide triphosphates (dNTPs), random primers (pdN_6) sodium salt, and klenow were from Pharmacia Biotech (Piscataway, NJ, USA). Autoradiography film, X-OMAT AR was from Kodak (Rochester, NY, USA). In vitro transcription was performed using the MEGAscript kit from Ambion (Austin, TX, USA).

H_2O used for all purposes is distilled, deionized and autoclaved.

3.2. Disposable materials

Polypropylene screw cap tubes (13 ml) were from Sarstedt (order #60.541, Newton, NC, USA). RNase-free 0.5 ml microfuge tubes were from United Scientific Products (San Leandro, CA, USA). Supported nitrocellulose membranes were from Schleicher and Schuell (Keene, NH, USA). Bio-Spin 30 columns were from Bio-Rad Laboratories (Hercules, CA, USA). Kapak tubular roll stock for heat seal bags was from BioWorld (Dublin, OH, USA).

3.3. Special equipment

The IS-1000 Digital Imaging System from Alpha Innotech (San Leandro, CA, USA) was employed to measure relative densitometric units. Agarose gel electrophoresis apparatus was constructed by Biomedical Engineering (LSUMC, New Orleans, LA, USA). Power supply was from EC Apparatus (St. Petersburg, FL, USA). A Sorvall RC-5B high speed centrifuge and SS-34 rotor were employed for RNA pelleting. The dot blot apparatus used was the Manifold I from Schleicher and Schuell (Keene). Dounce homogenizers were purchased from Kontes Glass (Vineland, NJ, USA). Nucleic acid concentrations were measured using a Perkin Elmer (Norwalk, CT, USA), Lambda Bio UV/Vis/NIR spectrometer. The geiger counter was from Mini-Instruments (Essex, England).

3.4. Solutions

(a) DEPC–H_2O: add 1 ml of DEPC to 1 l of H_2O. Shake vigorously. Loosen cap, place at 37°C. Shake vigorously several times over the next 3 h. After 12 h (or more) of incubation (can be left overnight), autoclave 15 min, liquid cycle.

(b) DEPC-treated solutions: treat as with H_2O. Some solutions are made and then DEPC-treated. Others are merely made using DEPC–H_2O.

(c) 2 M sodium acetate: should be treated with DEPC as is the DEPC–H_2O described above. Should be pH $\sim$ 4.

(d) Guanidine thiocyanate: to 100 g, add 119 ml of DEPC–H_2O, 4 ml of 1 M sodium citrate, pH 7 (DEPC-treated), 10.6 ml of 10% sarkosyl made using DEPC–H_2O.

(e) Water-saturated phenol: remove phenol from freezer, warm to room temperature, melt at 68°C. Add an equal volume of water, mix thoroughly. Remove water, repeat twice. Phenol is now ready to use (keep for at least 1 month at 4°C).

(f) Tris-saturated phenol: remove phenol from freezer, warm to room temperature, melt at 68°C. Add an equal volume of 1 M Tris, pH 8 and mix thoroughly. Remove the aqueous layer. Repeat twice. Add an equal volume of 0.1 M Tris pH 8 and mix thoroughly. Remove aqueous layer. Repeat (usually once) until pH is > 7.6. Phenol is now ready to use and may be stored for 1 month at 4°C.

(g) 100 × Denhardts: bring 10 g ficoll, 10 g polyvinylpyrrolidone and 10 g BSA up to 500 ml with water.

(h) 20 × SSC: add 175.3 g NaCl, 88.2 g sodium citrate and 800 ml of water. pH to 7 and adjust volume to 1 l.

(i) Prehybridization solution: for 100 ml, combine 50 ml of formamide, 5 ml of 1 M sodium phosphate, 10 ml of 10% glycine, 25 ml of 100 × Denhardts, 5 ml of 5 mg/ml salmon sperm DNA (boiled immediately prior to use), and 5 ml of 5 × SSC.

(j) Hybridization solution: for 20 ml, combine 10 ml of formamide, 0.4 ml of 1 M sodium phosphate, 0.2 ml of 100 × Denhardts, 0.4 ml of 5 mg/ml salmon sperm DNA (boiled immediately prior), 4 ml of 50% dextran sulfate, 4.2 ml of 20 × SSC, and 0.8 ml of radiolabeled probe in water (boiled immediately prior).

4. Detailed procedure

4.1. In vitro transcription (control)

A control experiment was performed to demonstrate linearity of hybridization within the model. Increasing amounts of in vitro transcribed p53 RNA were added to 0-h time point cerebral RNA. Double-strand radiolabeled cDNA was generated from the RNA and hybridized to nitrocellulose filter-fixed p53, IGF-1, transferrin receptor and bFGF. The latter three plasmids serve as controls and were applied at 5 μg per dot.

RNA was transcribed from 1 μg of Acc I digested p53/BS using T3 RNA polymerase to generate a run-off product < 1400 bp in length. p53/BS was generated by digestion of pHp53B with Bam HI and ligation into Bam HI-digested BS SK-II (BS SK-II is from Stratagene, La Jolla, CA, USA). In vitro transcription was performed using the MEGAscript kit according to the enclosed instructions. The run-off reaction proceeded for 3 h at 37°C. RNA was recovered by phenol:chloroform extraction (1:1) followed by chloroform extraction. RNA was precipitated by adding an equal volume of isopropanol in the presence of ammonium acetate. RNA concentration was determined by spectrophotometry and transcription product integrity was determined by product electrophoresis on a 0.8% denaturing agarose gel.

4.2. RNA isolation

We use a modification of the acid–phenol method of Chomczynski and Sacchi [3]. Brain cortex is rapidly isolated on an ice-cold dissecting board (other brain subsections may be isolated as desired). Tissue from each hemisphere is transferred to a cold dounce homogenizer. Materials and solutions are kept cold at all times.

(a) Add 5 ml of guanidine thiocyanate and homogenize tissue using 15 full strokes of the pestle. Apply additional strokes if needed until a milky homogeneous suspension is obtained.

(b) Transfer the homogenate to a screw cap Sarstedt tube.

(c) Add 500 μl of 2 M sodium acetate and invert several times to mix.

(d) Add 5 ml of water-saturated phenol and invert several times rapidly to mix.

(e) Add 1.5 ml of chloroform:isoamyl alcohol (49:1). Mix by rapid inversion for 10 s. Place at 4°C for 10 min.

(f) Centrifuge at 9000 rpm in SS-34 rotor with rubber adaptors (to prevent tube breakage); 4°C for 10 min.

(g) Remove upper phase without disturbing the interphase and transfer to a new 13 ml Sarstedt tube. Add an equal volume of isopropanol to precipitate the RNA. Place at −20°C for 30 min or until ready to proceed with the remainder of the procedure.

(h) Collect RNA by centrifugation as in (f). Do not permit the pellet to dry completely.

(i) Re-suspend the pellet in 0.2 ml of DEPC–H_2O. Re-suspend as rapidly as possible. Use mild vortexing intermittent with manual agitation to re-suspend pellet.

(j) Add 0.2 ml of guanidine thiocyanate. Transfer solution to 0.5 ml microfuge tubes.

(k) Add 0.1 ml of Tris-saturated phenol and 0.1 ml of chloroform:isoamyl alcohol (49:1). Vortex briefly and centrifuge 12,000 rpm for 5 min to separate phases.

(l) Transfer upper phase to a new microfuge tube. Repeat (k).

(m) Add 2 volumes of 95% ethanol, mix by inversion and centrifuge at 12,000 rpm for 10 min to pellet RNA.

(n) Wash pellet with 70% ethanol. Specifically, add 1 ml of 70% ethanol, shake or vortex until pellet is free-floating (pellet will not dissolve). Centrifuge for 5 min at 12,000 rpm to pellet. Remove ethanol and re-suspend in DEPC–H_2O. The amount of water will depend upon the amount of starting tissue. RNA yield from an adult rat brain is about 1 mg. Therefore, the RNA from one hemisphere may be suspended in 0.5 ml. Spectrometrically determine the concentration of RNA by reading 2 μl of the preparation in 1 ml of H_2O (1 OD_{260} unit is $\sim$40 μg of RNA). The 260/280 ratio should be 1.7–2.0. If ratio is higher than 2.0, ethanol precipitate again as in (m) and spectrometrically read the sample again.

(o) Aliquot 50 μg of RNA into each of several tubes. Add 0.1 volume of 2 M sodium acetate and 2 volumes of 95% ethanol, mix by inversion. Freeze at −70°C until ready to proceed. RNA should be stable for several years.

4.3. Preparation of probe

(a) Centrifuge RNA samples in ethanol at 12,000 rpm for 10 min in order to pellet RNA. Re-suspend the 50 μg pellets at 1 $\mu g/\mu l$ in DEPC–H_2O. Add to 5 μl of oligo dT (0.5 $\mu g/\mu l$). Heat to 70°C for 10 min, then place on ice.

(b) Prepare Master Mix 1. This mix will be distributed to each of the RNA preparations. Therefore, the volumes indicated should be multiplied by the number of reactions. For each reaction, add: 20 μl of 5 × First Strand Buffer, 10 μl of 0.1 M DTT, 5 μl dNTPs (a mix 10 mM with respect to dATP, dCTP, dGTP and dTTP), and 5 μl of [α-^{32}P]dCTP.

(c) Distribute 40 μl to each of the primed RNA mixtures. Mix by manual agitation, pulse centrifuge. Place at 37°C for 2 min. Add 10 μl of reverse transcriptase (200 $\mu/\mu l$). Incubate for 2 h at 37°C, then place on ice.

(d) Electrophorese 1 μl of the reaction mix on a 1% agarose gel with 1 μg of 1 kb ladder as size marker. Expose to film for 1 h. The labeled cDNA strands should fall in the 0.3–2 kb range. Continue with step (e) during the gel electrophoresis.

(e) Add 2 μl of pdN_6 (5 $\mu g/\mu l$ in H_2O) to each reaction tube. Place in a 90°C water bath for 10 min then on ice for 5 min.

(f) Prepare Master Mix 2. This mix will be distributed to each of the RNA preparations. For each reaction, add: 5 μl of 0.5 mM dNTPΔdCTP (dNTPs without dCTP), 15 μl of 10 × klenow buffer (we use New England Biolabs Buffer, NEBuffer #2; 10 × = 500 mM NaCl, 100 mM Tris–HCl, 100 mM $MgCl_2$, 10 mM DTT, pH 7.9), 10 μl of [α-^{32}P]dCTP and 5 μl of klenow (1 $\mu/\mu l$).

(g) Distribute 35 μl to each reaction, mix, pulse centrifuge. Incubate at 37°C overnight.

(h) Bring up to a final volume of 200 μl with TE pH 8 and centrifuge through a Bio-Spin 30 column according to manufacturer's instructions.

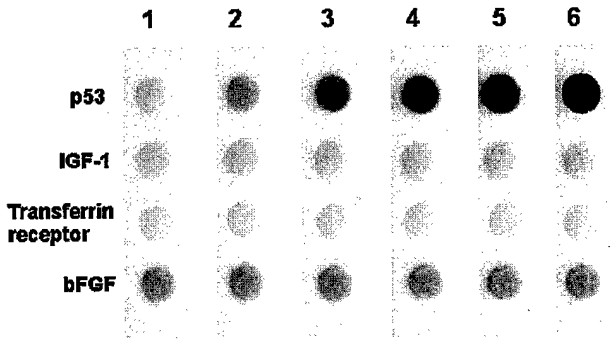

Fig. 1. p53 in vitro transcribed RNA was added to 0 h cerebral RNA and resulting radiolabeled cDNA products were hybridized to nitrocellulose filter-fixed clones. p53 RNA was added at 0.5, 1, 2, 4 and 8 ng, for hybridizations to filters 1–6, respectively.

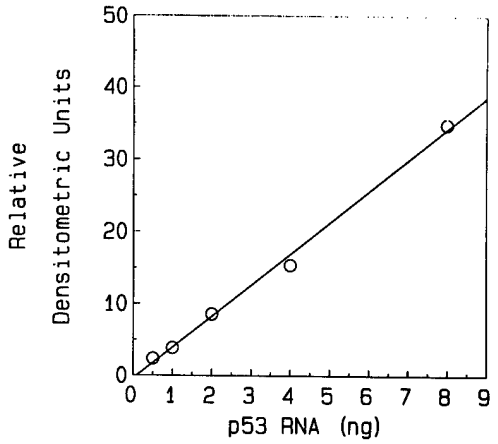

Fig. 2. Densitometric evaluation of p53 signals presented in Fig. 1.

4.4. Membrane preparation

The present study included the following plasmids: human somatostatin (81% identical to rat, ATCC 65122), human TK (85% identical to rat, ATCC 79803), mouse IGF-1 (ATCC 63070), and mouse c-*fos* (ATCC 41041). These were obtained from American Type Culture Collection (Rockville, MD, USA). The mouse GFAP clone in BSSK + was a gift of Nancy Nichols (USC, Los Angeles, CA, USA). The mouse Ren-2 cDNA is from Ken Gross (Roswell Park Mem. Inst., NY, USA). The MBP and PLP plasmids were pMBP-1 [7], 1.45 kbp rat myelin basic protein cDNA, and p27 [5], a 3019 bp cDNA clone of rat PLP in pUC18. Controls were pUC19 and pBR322 (New England Biolabs, Beverly, MA, USA).

Digest an amount of plasmid sufficient for 5 μg for each plasmid dot. Restriction enzymes should be chosen which linearize the plasmid (an enzyme which cleaves at multiple sites may also be used). The following procedure is sufficient to prepare plasmid for application to five blots. (a) Digest 25 μg of plasmid in a 30-μl digest. Plasmids without inserted cDNAs should be included as controls (preferably plasmids in which the cDNAs of interest are ligated). (b) Add 25 μl of water and 6 μl of fresh (< 2 weeks old) 1 M sodium hydroxide. Incubate for 30 min at room temperature. (c) Add 0.6 ml of 6 × SSC. (d) To prepare nitrocellulose, immerse in water until completely wet. Transfer to a dish containing 6 × SSC and wet thoroughly. Assemble on the manifold according to Schleicher and Schuell directions. (e) Apply 125 μl of the material from (c) to each of five dots on five consecutive blots. Rinse each slot with 500 μl of 6 × SSC. (f) Remove membrane with underlying filter paper and UV crosslink using program C3 (150 mJ). Membrane should be damp for this program. (g) Transfer the membrane to 3MM paper and permit to dry. Wrap in aluminum foil and plastic wrap and store in a cool dry drawer until ready to proceed.

4.5. Prehybridization and hybridization

The membrane is placed in tube roll plastic, cut to size and heat sealed. A 10 ml of prehybridization solution is added and incubated at 42°C for 4–6 h. Following prehybridization, the solution is removed through a slit in the corner of the bag and the hybridization solution is delivered using a 10-ml pipet. The bag is then resealed. We use $5–10 \times 10^6$ cpm/ml of hybridization solution. All time points in a given comparison should be hybridized with the same amount (cpm) of radioactive probe for a period of at least 24 h at 42°C. (a) Wash filter in 500 ml of 2 × SSC, 0.1% SDS at room temperature for 30 min. (b) Repeat. (c) Repeat wash sequence at 50°C. (d) Finally, wash membranes twice at 50°C in 0.1 × SSC, 0.1% SDS for 15 min (for heterologous probes or at 65°C in 0.1 × SSC, 0.1% SDS for 15 min (for homologous probes).

Filters may be monitored by Geiger counter. Damp films are placed on waterproof supports (we use outdated autoradiography film), covered with saran wrap and exposed to film for 48–72 h depending on the strength of the signal (as determined by Geiger counter). Films are then examined and dots quantified using the IS-1000 digital imaging system. Multiple exposures may be required if all signals are not within the linear range of instrument detection and quantification.

4.6. Statistics

Statistical analyses were performed using a one-way analysis of variance (ANOVA) followed by a Dunnett Multiple Comparisons post-hoc test.

5. Results

The present study reports a partial time-course of expression of various mRNAs in cortex following injury. Nitrocellulose filter-fixed probes were hybridized to radiolabeled cDNAs generated from cortical RNAs. A pilot study was performed to test for linearity of the model. p53 RNA was transcribed in vitro and quantities between 0.5 and 8 ng were added to 0 h control RNA prior to reverse

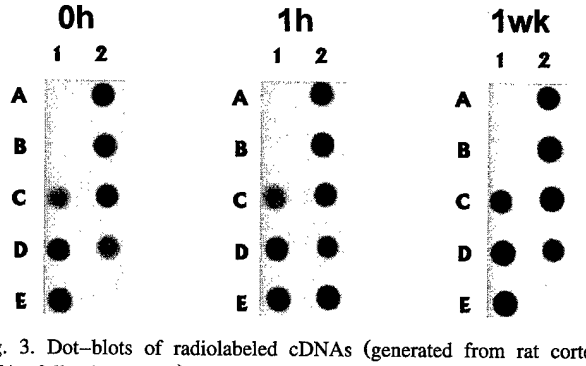

Fig. 3. Dot–blots of radiolabeled cDNAs (generated from rat cortex RNAs following injury) hybridized to nitrocellulose filter-fixed clones. 1A, pUC19; 1B, pBR322; 1C, somatostatin; 1D, MBP; 1E, PLP; 2A, GFAP; 2B, TK; 2C, IGF-1; 2D, renin; 2E, c-*fos*.

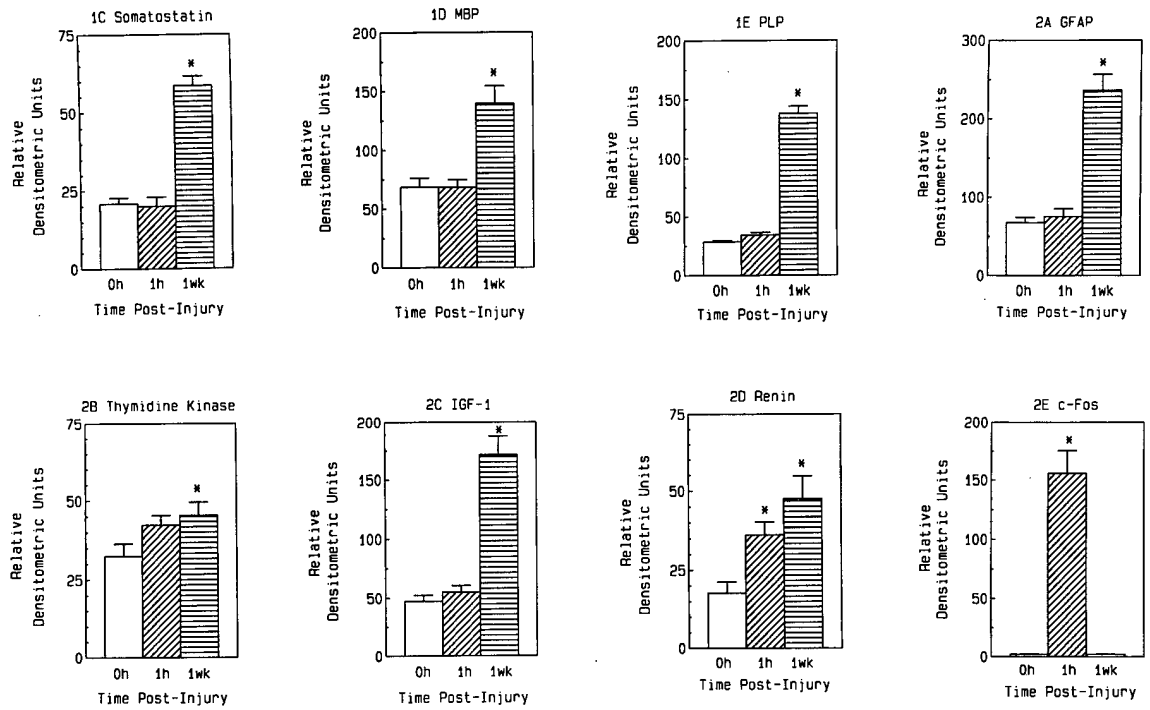

Fig. 4. Graphical illustrations of cortex-derived radiolabeled cDNAs bound to filter-fixed clones, as a function of time post-injury. Bars represent mean and standard deviation of three unrelated experiments. Asterisks indicate values significantly greater than 0 h control, $P < 0.05$.

transcription. The resulting radiolabeled double-strand cDNAs were hybridized to filter-fixed p53 and controls (Fig. 1). The hybridization signals were quantified by densitometry and plotted in Fig. 2. The system is clearly linear over a significant and relevant range.

RNAs were collected at 0 and 1 h, and 1 week following cryogenic injury. RNAs were also collected from sham-operated animals at 0 h post-injury. In no case was the hybridization signal obtained from the sham-operated rats significantly different from that of the 0 h control. For each time point, RNAs from three rats were collected and analyzed. Each panel within Fig. 3 represents one of three independent experiments. Fig. 4 is a graphical presentation of the hybridization signals (mean ± standard deviation) obtained from the three independent experiments for each time point. Since significant hybridization signals were not obtained for pUC19 and pBR322 (positions 1A and 1B, Fig. 3) they are not graphically represented.

We feel it important to caution the reader about comparing the absolute values of hybridization signals obtained from different filter-fixed probes. The absolute densitometric value (hybridization signal) for a given filter-fixed DNA is dependent upon the length of the homology, the extent of the homology (species-specificity of the filter-fixed DNA), and the hybridization conditions.

6. Discussion

A number of studies have addressed the expression of neural factors (growth, differentiation, and trophic factors) following brain injury. These studies have generally examined the corresponding protein and/or mRNA of a single gene and variably employ ischemia, trauma, or cryogenic wounds. Since the nature of the wound may itself influence the time course of expression and the maximum expression of a given gene, it is difficult to consolidate these studies in order to determine the relative time course of expression of multiple genes during wound healing.

In the present study, we simultaneously examined the expression of eight genes at two different time points following injury. We employed a cryogenic injury model which we had previously used to study the effects of injury and dexamethasone on fatty acid accumulation and edema [1,6]. A modification of the method of Chalifour et al. [2] was employed to study gene expression. Double-stranded, radiolabeled cDNAs, transcribed from RNAs collected at each time point, were hybridized to filter-bound plasmids possessing inserted mammalian DNAs of interest. A more detailed study of changes in the expression of these eight genes together with 10 additional genes is presented elsewhere [4]. In the latter study, 18 different genes are concurrently examined at eight different time points following injury. This method is reliable for quantitative assessment of RNAs present at abundant to modest levels. Quantification of rare transcripts requires more sensitive methods such as quantitative PCR or RNase protection.

This study furnishes insight into the sequence of genetic events that follow brain injury, many of which may contribute to the wound-healing process. Knowledge of the stepwise events controlling wound healing following brain

injury should contribute to the tailored treatment of affected patients. Administration of peptides or drugs which induce or repress peptide expression may optimize healing and minimize excessive scar tissue formation. As gene therapy techniques become increasingly sophisticated and efficient, expression plasmid, viral vector, or oligonucleotide administration may become commonplace strategies. Treatments may be most effective if tailored to specific forms of injury or to specific regions of the brain. Regardless, effective treatment of brain injuries with drugs, peptides or genes will require a thorough understanding of the complex cellular changes and inter-cellular interactions which occur following insult.

7. Troubleshooting

7.1. Poor recovery of radiolabeled double-stranded cDNA

Occasionally, for reasons that are unclear to us, we do not quantitatively recover the cDNA from the Biospin 30 columns. This may reflect a problem with specific batches of column matrix, or with the age or storage conditions of the columns. In such cases, we find that we can add to the mixture from Section 4.2 (g), an equal volume of TE pH 8, one-tenth volume of 2 M sodium acetate and 2 volumes of ethanol to precipitate the DNA and remove most of the unincorporated radioisotope (which can increase background).

7.2. Poor hybridization despite satisfactory yields of high specific activity probe

The corresponding RNA may simply be present at very low levels. Phosphorimage analysis may permit quantification of low level hybridizations and may also allow comparison of signals over a very broad range due to linearity properties.

8. Quick procedure

1. Extraction of RNA from tissue or cells.
2. Reverse transcription of RNA.
3. Second strand synthesis to produce radiolabeled product.
4. Hybridization to membrane-bound probes.
5. Quantification of signals using digital imaging.

Acknowledgements

This work was supported by grant DAMD17-93-V-3013 from the Department of Defense.

References

[1] N.G., Bazan, E. Politi, E.B.R. de Turco, Endogenous pools of arachidonic acid-enriched membrane lipids in cryogenic brain edema, in: K.G. Go, A. Besthmann (Eds.), Recent Progress in the Study and Therapy of Brain Edema, Plenum, 1984, pp. 203–212.

[2] L.E. Chalifour, R. Fahmy, E.L. Holder, E.W. Hutchinson, C.K. Osterland, H.M. Schipper, E. Wang, A method for analysis of gene expression patterns, Anal. Biochem. 216 (1994) 299–304.

[3] P. Chomczynski, N. Sacchi, Single-step method of RNA isolation by acid guanidinium thiocyanate–phenol–chloroform extraction, Anal. Biochem. 162 (1987) 156–159.

[4] J.L. Cook, V. Marcheselli, J. Alam, P.L. Deininger, N.G. Bazan, Temporal changes in gene expression following cryogenic rat brain injury, Mol. Brain Res., in press, 1998.

[5] R.J. Milner, C. Lai, K.-A. Nave, D. Lenoir, J. Ogata, J.G. Sutcliff, Nucleotide sequences of two mRNAs for rat brain myelin proteolipid protein, Cell 42 (1985) 931–939.

[6] L.E. Politi, R. De Turco, N.G. Bazan, Dexamethasone effect on free fatty acid and diacylglycerol accumulation during experimentally induced vasogenic brain edema, Neurochem. Pathol. 3 (1985) 249–269.

[7] A. Roach, K. Boylan, S. Horvath, S.B. Prusiner, L.E. Hood, Characterization of cloned cDNA representing rat myelin basic protein: absence of expression in brain of shiverer mutant mice, Cell 34 (1983) 799–806.

Elsevier Science

Fax: (31) (20) 485 3271
Phone: (31) (20) 485 3435

Postal Address:
Brain Research
Elsevier Science
P.O. Box 2759, 1000 CT Amsterdam
The Netherlands

Courier Service Address:
Brain Research
Elsevier Science
Sara Burgerhartstraat 25, 1055 KV Amsterdam
The Netherlands

* * *

If you need information about your accepted manuscript, proof, etc. then phone or FAX us at the above numbers, stating the journal name and article code number. We can FAX this journal's Instructions to Authors to you which can also be found on the World Wide Web: access under http://www.elsevier.com

SUBSCRIPTION AND PUBLICATION DATA 1998

Brain Research (including **Molecular Brain Research, Developmental Brain Research, Cognitive Brain Research, Brain Research Protocols** and **Brain Research Reviews**) will appear weekly and be contained in 59 volumes (125 issues): **Brain Research, Volumes 779–814** (36 volumes in 72 issues), **Molecular Brain Research, Volumes 51–61** (11 volumes in 22 issues), **Developmental Brain Research, Volumes 105–111** (7 volumes in 14 issues), **Cognitive Brain Research, Volume 6** (1 volume in 4 issues), **Brain Research Protocols, Volume 2** (1 volume in 4 issues) and **Brain Research Reviews, Volumes 26–28** (3 volumes in 9 issues). Please note that **Volumes 51–52** of **Molecular Brain Research, Volume 6** (Issues no. 1 and 2) of **Cognitive Brain Research** and **Volume 2** (Issue no. 1) of **Brain Research Protocols** were published ahead of schedule in 1997, in order to reduce publication time. The volumes remain part of the 1998 subscription year.

Separate subscriptions: Molecular Brain Research, Vols. 51–61, Developmental Brain Research, Vols. 105–111, Cognitive Brain Research, Vol. 6, Brain Research Protocols, Vol. 2 and **Brain Research Reviews, Vols. 26–28,** may also be ordered separately. Prices are available from the Publisher upon request. Subscriptions are accepted on a prepaid basis only, unless different terms have been previously agreed upon.

Postage and handling charges include surface delivery except to the following countries where air delivery via SAL (Surface Air Lift) mail is ensured: Argentina, Australia, Brazil, Canada, Hong Kong, India, Israel, Japan, Malaysia, Mexico, New Zealand, Pakistan, P.R. China, Singapore, South Africa, South Korea, Taiwan, Thailand and USA. For all other countries airmail rates are available upon request.

Claims for missing issues must be made within six months of our publication (mailing) date, otherwise such claims cannot be honoured free of charge. **Orders, claims, and product enquiries:** please contact the Customer Support Department at the Regional Sales Office nearest to you: **New York**, Elsevier Science, P.O. Box 945, New York, NY 10159-0945, USA. Tel: (+1) 212-633-3730, [Toll free number for North American customers: 1-888-4ES-INFO (437-4636)], Fax: (+1) 212-633-3680, E-mail: usinfo-f@elsevier.com. **Amsterdam**, Elsevier Science, P.O. Box 211, 1000 AE Amsterdam, The Netherlands. Tel: (+31) 20-485-3757, Fax: (+31) 20-485-3432, E-mail: nlinfo-f@elsevier.nl. **Tokyo**, Elsevier Science, 9-15, Higashi-Azabu 1-chome, Minato-ku, Tokyo 106-0044, Japan. Tel: (+81) 3-5561-5033, Fax: (+81) 3-5561-5047, E-mail: info@elsevier.co.jp. **Singapore**, Elsevier Science, No. 1 Temasek Avenue, #17-01 Millenia Tower, Singapore 039192. Tel: (+65) 434-3727, Fax: (+65) 337-2230, E-mail: asiainfo@elsevier.com.sg. **Rio de Janeiro**, Elsevier Science, Rua Sete de Setembro 111/16 Andar, 20050-002 Centro, Rio de Janeiro - RJ, Brazil. Tel: (+55) (21) 509 5340; Fax: (+55) (21) 507 1991; E-mail: elsevier@campus.com.br [Note (Latin America): for orders, claims and help desk information, please contact the Regional Sales Office in New York as listed above].

Advertising information: Advertising orders and enquiries can be sent to: **Europe and ROW:** Rachel Gresle-Farthing, Elsevier Science Ltd., Advertising Department, The Boulevard, Langford Lane, Kidlington, Oxford OX5 1GB, UK. Tel: (+44) (1865) 843565; Fax: (+44) (1865) 843976;E-mail: r.gresle-farthing@elsevier.co.uk. **USA and Canada:** Elsevier Science Inc., Mr. Tino DeCarlo, 655 Avenue of the Americas, New York, NY 10010-5107, USA. Tel: (+1) (212) 633 3815; Fax: (+1) (212) 633 3820; E-mail: t.decarlo@elsevier.com. **Japan:** Elsevier Science KK, Advertising Department, 9-15 Higashi-Azabu 1-chome, Minato-ku, Tokyo 106-0044, Japan. Tel: (+81) (3) 5561-5033; Fax: (+81) (3) 5561 5047.

ADONIS Identifier. This Journal is in the **ADONIS** Service, whereby copies of individual articles can be printed out from CD-ROM on request. An explanatory leaflet can be obtained by writing to **ADONIS** B.V., P.O. Box 17005, 1001 JA Amsterdam, The Netherlands.

♾ The paper used in this publication meets the requirements of ANSI/NISO Z39.48-1992 (Permanence of Paper).

PROJECT 2. PATHOPHYSIOLOGICAL EVENTS TRIGGERED DURING LIGHT-INDUCED DAMAGE TO THE RETINA.

1 INTRODUCTION

Very intense and/or prolonged light will damage photoreceptor cells. Rod photoreceptors are most susceptible and under extraordinary conditions can be totally lost. Cone photoreceptors suffer less damage to bright light, but require the presence of rods for normal maintenance and function. Loss of rods, then, can eventually lead to cone photoreceptor loss as well.

There are two mechanisms through which cells die. The first, *necrosis*, involves some compromise of the cell's integrity, with physical alterations occurring in the plasma membrane. Ionic imbalances then occur, favoring swelling and cell rupture. Components are rapidly degraded and removed. Necrosis can be initiated through a variety of ways that include bacterial and viral infections, as well as simple physical damage.

The second mechanism, *apoptosis*, is more subtle, occurring from within the cell itself. A cascade of events is triggered that ultimately results in the production of endonucleases, DNA-cleaving enzymes that target specific sites within the nucleus. When present, these enzymes break DNA at very regular intervals along the nucleosomes, reducing it to many useless fragments of multiples of 180-200 base pairs (the length of intranucleosomal stretches), killing the cell (Oberhammer et al., 1993). Cells dying by apoptosis retain their integrity, appearing intact with normal organelles; in effect, the nucleus is shut down.

Apoptosis is a normal component of both development and tissue maintenance in the mature organism, but can be inappropriately triggered

by pathophysiological stimuli. Because apoptotic cells retain their membrane integrity, they are usually phagocytized before lysis occurs. Therefore, nearby cells are not damaged by the release of lytic enzymes, and an inflammatory response is not triggered. This contrasts with necrosis and its accompanying inflammation. Excessive amounts of light trigger the process of apoptosis in photoreceptor cells.

We have previously explored the steps leading to the onset of apoptosis. When appropriately stimulated, phospholipase A_2 (PLA_2), the enzyme responsible for the release of arachidonic acid (AA), is activated within1-2 minutes. The induction of prostaglandin G/H synthase-2 (cyclo-oxygenase-2; COX-2), an isoform of the enzyme that catalyzes the rate-limiting step in the biosynthesis of prostagladins and thromboxanes and the conversion of AA to prostaglandin H_2, follows. COX-2 protein levels are low and don't begin to elevate for 2-3 hours, peaking 6-8 hours after stimulus. COX 2 has been localized in both endoplasmic reticulum and nuclear membranes (Morita et al., 1995; Coffey et al., 1997), and in post-synaptic dendritic formations in neurons (Kaufmann et al, 1996), and may also be responsible for the synthesis of prostanoids involved in nuclear signaling events. COX 2 is activated as a result of several forms of neurological insult (Marcheselli and Bazan, 1996; Bazan et al, 1996; Yamagata et al, 1993; Miettinen et al, 1997) and we have strong evidence that COX 2 is induced in our light damage model.

When AA is released by PLA_2, the remaining molecule, lyso-platelet activating factor (lyso-PAF) is converted to PAF by PAF-acetyltransferase. We have shown that PAF is an activator of COX 2 expression *in vitro* (Bazan et al, 1994) and *in vivo* (Marcheselli and Bazan, 1996), and that the presence of a PAF receptor antagonist inhibits light-induced COX-2 induction and retinal damage (Reme, 19). Thus, anything that blocks

COX-2 induction should inhibit light-induced apoptosis and photoreceptor cell loss. Similarly, anything that promotes PAF removal should prevent or reduce light damage.

When PAF is formed, it is rapidly converted back to lyso-PAF by PAF-acetylhydrolase (PAF-AH). This enzyme is composed of three subunits, the α1 (29 KDa) and the α2 (30 KDa) catalytic subunits and the β (45 KDa) regulatory subunit. We now have two lines of transgenic rats that overexpress these subunits; CAMKII-30 which has the α2 catalytic subunit associated with a Calmodulin Kinase IIα promoter, and NSE-45 which has the β regulatory subunit associated with a Neuron Specific Enolase promotor. These lines are providing us with the extraordinary opportunity to study the effect of excessive light on retinas that overexpress these subunits, and, thus, reduce the availability of PAF for the induction of COX-2 and subsequent apoptosis.

Exquisitely sensitive techniques are now available that allow labeling of the tips of DNA fragments. This TUNEL method of labeled nicked DNA produces images of damaged nuclei that fluoresce a brilliant yellow-green, allowing analysis of the sectioned tissue. In the first part of this study, this histological procedure has been utilized to study the effects of bright light on the retinas of the CAMKII-30 and NSE-45 transgenic rat lines.

Finally, it is important to consider the remaining portion of the apoptotic mechanism. How is it that the over abundance of COX-2 triggers cell death? When COX-2 adds oxygen to AA to cyclicize it and form the prostaglandin precursor, free radicals are formed. The presence of these free radicals can strongly affect mitochondria. This is especially important in photoreceptors because mitochondria within the inner segment are bunched into a tight mass, the ellipsoid, which resides just below the outer

segment. In effect, this localizes all mitochondria close to where COX-2 is being synthesized, and this may be the heart of the problem.

There are two groups of proteins that are known to be involved in the process of apoptosis. These are the members of the bcl-2 protein family, which are cytoplasmic, and cytochrome-c, a mitochondrial compound. bcl-2 performs a protective role by forming homodimers that bind to the mitochondrial membrane, preventing cytochrome-c from entering the cytoplasm. bcl-X_L also appears to be able to bind to cytochrome-c, preventing mobilization (Duckett et al., 1998). When COX-2 catalyzes the conversion of AA to a prostaglandin, free radicals are formed, and an over abundance of free radicals decreases the levels of the bcl proteins. Loss of these compounds allows cytochrome-c to leave the mitochondria, which then results in two things. First, the mitochondrial membrane potential is lost (cytochromes are charged molecules functioning in the electron transport chain), which could compromise normal mitochondrial function (Schulze-Osthoff et al., 1992). Second, once cytochrome-c arrives in the cytoplasm, it activates caspases, a family of proteases that exist in an inactive state (Kitamura et al., 1998; Zou et al., 1997). Caspases act on the histones that surround the DNA, causing enough damage that endonucleases can enter and fragment the DNA along the nucleosome chains.

In the second part of this study we have monitored levels of COX-2, bcl-2, bcl-K_L, and cytochrome-c protein levels, in the presence of a PAF receptor antagonist, with Western blot analysis at 8 hr and 24 hr after light treatment to determine if this mitochondrial mechanism is involved in triggering photoreceptor cell loss.

2 BODY

A Previous Work

In previous years (years 1-3) we have used two models of light damage to rat retinas, long-term exposure to moderately-damaging light (300 lux, 6 days cycled light, or 1400 lux, 3 days of cycled light), and a short-term exposure to more intense light (7000 lux, 2 hours). In both models light was delivered from above the animals. We have performed detailed histological studies showing that our protocols induce rod photoreceptor apoptosis and cell loss with a temporal and spatial pattern characteristic of light delivered from above, with most damage occurring in the inferior-nasal quadrant of the retina. We also used Western blotting and immunohistochemistry to demonstrate light induction, in the intense light model, of COX-2, and to show that the PAF antagonist BN-50730 blocked this action.

We extended our rat model of light damage to include circular stimulation, essentially surrounding the animal with fluorescent lights. These stimulators also supplied 7000 lux over a 2 hr period. Comparisons between superior horizontal stimulation and circumferential stimulation were made and the circular model was found produce more consistent results.

We established a time course of retinal light damage-induced apoptosis using the 7000 lux model and demonstrated the peak of apoptosis at 20-24 hrs after stimulation. Light damage and the effects of PAF receptor blockers were assessed histologically by the TUNEL reaction, and we determined that BN-50730 did reduce the light induction of COX-2. In addition to TUNEL staining, we utilized an ELISA method based on the release of mono- and poly-oligosomes from nuclear chromatin to demonstrate apoptosis and the protective effects of BN-50730.

B Objectives, Year 5

During the present project period, we extended our previous findings of the pathophysiological events triggered during light-induced damage to the retina to a transgenic model of rats over expressing the β (45 kDa) regulatory and α2 (30 kDa) catalytic PAF-AH subunits.

In order to investigate the effects of PAF acetylhydrolase subunits on second messengers, we constructed different lines of transgenic rats overexpressing the three subunits (α1, α2, and β) under control by the NSE and CAMKII promoters. Two lines overexpressing the β (45 kDa) subunit and α2 (30 kDa) subunit, respectively, in the retina were used. These animals were light damaged for 5 hrs at 7000 lux in the circular light source and then analyzed histologically by the TUNEL technique.

Finally, using Western blot analysis, we determined the levels of bcl proteins, cytochrome-c, and COX-2 in the presence and absence of a PAF receptor antagonist, following light treatment, to see if mitochondrial mechanisms were contributing to photoreceptor cell loss.

3 MATERIALS AND METHODS

Light Stimulation and Animal Treatment

The light stimulator consists of 8 circular fluorescent lights (G.E. cool white, 8" dia) mounted on end, 2" apart, center-to-center. A lucite tube containing the animals is placed through the center of these lamps where it remains for 2 or 5 hr. A cooling fan continually blows air through the animal tube. All animals were dark adapted for 3 days and then their pupils dilated just prior to light treatment. Following light exposure, they were returned to their cages and given food and water *ad libitum* until retinas were collected.

Tissue Processing and Histology

Retinas were to be viewed by the TUNEL method of labeled nicked DNA, as well as by conventional high resolution light microscopy.

Following 5 hr of light treatment, retinas were collected after 24 hr for TUNEL labeling. Eyes were slit and placed overnight in 10% neutral buffered formalin (Mallinckrodt, Paris, KY) at 4° C. Eyecups were prepared and then cut through the optic nerve along the superior-inferior axix. After an additional hour in fixative, the tissue was dehydrated through an ethanol series to xylene, and then paraffin. Embedded retinas were sectioned (10 μm thickness), floated on water, and affixed to glass slides. After removing paraffin, the TUNEL reaction was performed. The Promega (Madison, WI) TUNEL-labeling kit was used exactly as described in the kit protocol. Following this, propidium iodide was used as a nuclear counter stain. Sections were coverslipped in glycerol and viewed with fluorescence microscopy. TUNEL fluoresced yellow-green because of the presence of an FITC tag; all other nuclei fluoresced a dim red.

After 5 hr of light treatment, retinas were also collected after 8 days to determine if there had been permanent photoreceptor damage and cell loss. Corneas and lenses were removed. Eyecups were prepared and cut along the superior-inferior axis through the optic nerve and fixed in 2% formaldehyde and 2% glutaraldehyde in 0.135 M sodium cacodylate buffer, pH 7.4, at 4° C overnight. Following a buffer rinse in the same buffer, post fixation in 1% OsO_4 for 1 hr, and another buffer rinse, tissue was dehydrated through an ethanol series to acetone, infiltrated with an Epon/Araldite plastic mixture (Mollenhauer, 1963), and embedded. Sections (1 μm thick) were floated on water and affixed to glass slides. Slides were stained with 0.5% toluidine blue in 0.5% boric acid for 2 min on a hot plate. After rinsing and drying, sections were coverslipped temporarily

with glycerol and viewed with bright field microscopy.

Microscopy

Sections were viewed with a Nikon Optiphot-2 under epi-fluorescence with a fluorescein filter packet or with conventional bright field illumination. Images were detected with a SONY 3CCD color DXC-960MD camera and viewed on a SONY Trinitron color monitor at an initial magnification of 200x. Images were captured and digitized, and archiving and analysis accomplished by computer, utilizing Adobe Photoshop (Adobe Systems, Mountain View, CA) and Image Pro-Plus (Media Cybernetics, Silverspring, MD).

Analysis of TUNEL

The light from each successive 400 X microscope field was measured with an automatic metering system and the length of time (sec) for the correct exposure was recorded for each of the 33 retinal fields, for each of the rats. All measurements began at the superior edge, progressed across the optic nerve, and ended at the inferior edge. Thus, high TUNEL labeling (bright light) produced a small number, low or no label (dim light) resulted in a large number. When plotted linearly as a histogram, the resulting profile represented the extent of label across the retina. These field values were then normalized to 100% and retinas compared.

Transgene Construction

The transgenic PAF-AH lb subunit constructs were made using promoters designed to direct expression specifically in neurons. The promoters used were Neuron Specific Enolase(NSE) and Rat Calmodulin Kinase II alpha. The cDNA for the rat PAF-AH (a gift from Dr. Inoue) was cloned into the restriction site of EcoRV of the pNN265 vector and then removed along with the attached 573' intron plus poly A signal by digestion with Noti. The Noti

fragment was inserted into the Noti site of the pMM4O3 vector (CAMKII promoter) (a gift from Dr. Kandel). The entire CAMKII promoter/cDNA fusion was digested with Sf1 and removed for microinjection using Sprague-Dawley rats. Transgenic rats were generated by DNX (Princeton, NJ). The cDNA for the bovine PAF-AH lb was cloned into the NSE/PmT2 vector (a gift from Dr. Cook), digested with restriction enzymes, and purified for microinjection.

Quick Tail DNA Preparation for Genotyping

1-2cm rat tail was added to digestion buffer (5mM EDTA, 200mM NaCl, 100mM Tris-HCl (pH 8.0), 0.2% SDS), 0.5 mg/ml proteinase k, and 12.5 jig/ml ribonuclease A, and digested overnight in a water bath at 55°C. The DNA was extracted with phenol/chloroform/isoamyl alcohol and precipitated with 1:1 isopropanol. Pellets were resuspended in Tris-EDTA (pH 8) and heated for 2 hours at 65^0 C.

Genomic RT-PCR

All PCR reagents were from GIBCO-BRL (Gaithersburg, MD).

PCR was done as follows:

1 x PCR buffer, 1.5 mM $MgCl_2$,0. 1 mM dNTPs,400nM primers, water, and taq DNA polymerase (1 unit), in a total volume of 50 pl. PCR was carried out using a Perkin Elmer GeneAmp PCR System 9600 cycler with the following conditions: 94^0 C for 0.25 minutes, 55^0 C for 0.25 minutes, and 72^0 C for 0.5 minutes for 30 cycles. PCR product was analyzed on a 1.8% agarose gel. The tail DNA PCR was designed only to show if the animal carried the transgenic vector sequence. RT-PCR was required to indicate which of the transgenic PAF-AH subunit sequences were expressed.

Protocol for COX-2 Western-blotting of rat retinal tissue

Tissue samples are kept in ice until homogenization. Rapidly homogenize retinal tissue in a 2 ml glass-on-glass homogenizer with 0.5 ml of lysis buffer (10 mM Tris-HCl, 10 mM EDTA, 5mM EGTA, 1 % Triton-X-100, pH 7.4. Add protease inhibitors just before use: 0.1M PMSF, 0.1 TIU/ml aprotinin, and 0.1M leupeptin) at room temperature. Sonicate the homogenates for 30 seconds. Measure protein concentration on samples, and use lysis buffer aliquots on the standard curve and blanks to correct for protease inhibitors. Dilute proteins to a content of 10 µg proteins in 10 µl lysis buffer. Add to each sample an equal volume of 2 X concentrated electrophoresis sample buffer (250 mM Tris-HCl, pH 6.5, 2% SDS, 10% glycerol, 0.006% bromophenol blue, and 10 µl/ml mercaptoethanol). Keep samples on ice, but just before gel loading, boil samples for 3 - 5 min. The electrophoresis apparatus preparations and gel casting should be started before tissue homogenization. Load samples (20 µl/well) onto a 0.75 -1.00 mm thick SDS-polyacrylamide gel. Run at 180-200 volts, for 45-60 min. For gel transfer, soak the gel in ice cold transfer buffer (4°C) for 30 min to allow the gel shrink to final size and remove residual running buffer. Install gel and nylon membrane on transfer apparatus and start transfer at 100 V for1 hour. Disassemble the apparatus, remove membranes from the cassettes and, with a soft pencil, mark the position of main bands from molecular markers, labeling the side were the proteins are bound. Soak the membranes in blocking buffer overnight at 4° C, or for 30 min at 37° C on an oscillatory platform. Incubate at 37° C with the primary antibody for 30 min. Dilute the primary antibody in 10 ml of blocking buffer. Antibody dilutions are: PGHS-1, 1:2000 (Polyclonal Anti-PGHS-1) Cat.# M-20 Santa Cruz. PGHS-2, 1:2000 (Monoclonal Anti-PGHS-2) Cat.# 16011 Cayman. Bcl-2, 1:2000 (goat polyclonal antibody), Cat # N-19 Santa Cruz. Cytochrom-c, 1:2000 (mouse monoclonal antibody), Cat # 65981A Pharmingen. Bcl-X_L, 1:2000 (mouse monoclonal antibody), Cat # 66461AA

Pharmingen. Wash the membranes in fresh blocking buffer. Place membranes in weighing buckets with 25 ml blocking buffer at room temperature on a rocking platform. Each 5 min replace buffer and keep rocking until complete (30 min). Incubate membranes at 37° C with secondary antibody for 30 min in a rotatory oven. Dilute the secondary antibody in 10 ml blocking buffer, anti-mouse IgG, 1:2000 (anti-mouse IgG horseradish peroxidase conjugate) Catalog # M15345L3 Transduction Laboratories.

For alkaline phosphatase we use 1:10,000 dilution of secondary antibody. Wash membranes in blocking buffer. Place membranes in weighing boats with 25 ml blocking buffer at room temperature, on a rocking platform. Each 5 min replace buffer and keep rocking until complete (30 min).

4 RESULTS

Two lines of transgenic rats were used. The first exhibited overexpression of the β (45 kDa) subunit (regulatory) of PAF-AH under the direction of the NSE promotor, the second line demonstrated overexpression of the α2 (30 kDa) subunit (catalytic) of PAF-AH under the direction of the CAMKII promotor. After testing litter mates for the presence or absence of these subunits, 3 plus and 3 minus animals were selected from each transgenic line for light testing. The RT-PCR gels of these rats, demonstrating their genotype, are shown in **figure 1** (NSE) and **figure 2** (CAMKII).

TUNEL labeling at 24 hr post light treatment. At 24 hr post light treatment, all retinas showed evidence of DNA fragmentation. The NSE-45 retinas demonstrated only light damage, localized to a small region within the upper half of the retina, and both the plus and minus animals showed equivalent amounts of label. **Figure 3** represents a typical NSE-45 TUNEL

labeled retina. Labeling is sparse, with the nuclei only partially labeled. Because only the outer-most portions of the nuclei are labeled, fragmentation has not been extensive. Only photoreceptor nuclei have labeled. Within the region of labeling, only about 20% show damage. The inferior retina contains no labeled nuclei, indicating a superior region of higher susceptibility.

Retinas from the CAMKII-30 transgenic line demonstrated a very different profile. In all cases, both the plus and the minus retinas were extensively labeled. Dense label favored the superior retina, but extended into the inferior portion as well, and even the inferior-most regions had some scattered labeling. Within the dense superior region, 100% of the nuclei were TUNEL positive (**figure 4**). Moreover, the entire nucleus was labeled. Overall comparisons between the plus and minus retinas did not reveal differences in extent or intensity of label.

Some RPE cells were TUNEL positive in the CAMKII-30 retinas, but not in the NSE-45 samples. When RPE cells were positive they were intensely labeled. Also, both their nuclei and cytoplasm glowed (**figure 5**), probably indicating severe damage and nuclear breakdown. Damaged RPE cells were localized to the central portion of the TUNEL positive photoreceptor region.

Relative inverse light intensity measurements from successive fields across each retina are shown in **figure 6**. **Figure 7** shows these same values after having been normalized. Plots of these values illustrate the amount and extent of the DNA fragmentation across each retina. Both the plus and minus NSE-45 retinas showed very similar profiles (**figure 8**), with most of the retinas at background level. A shallow narrow notch was evident in the central superior region of each (**figure 8**, arrows).

TUNEL profiles for the CAMKII-30 retinas were very different. Both plus and minus retinas exhibited deep extensive DNA fragmentation that covered all the superior retina and extended well into the inferior portion. The minus retinas showed more extensive damage (approximately 20 % more) than the plus retinas (**figure 9**). All retinas in this line had labeled RPE cells. The distribution of these cells across each retina is shown as a bar under each of the retina plots. In general, the damaged RPE is centered behind the TUNEL positive photoreceptors and in the superior retina.

The area of the regions containing the fragmented DNA was calculated (**figure 10**). The amount of fragmentation is the same between the plus and minus NSE-45 retinas (17.9% and 16.8%, respectively). However, the CAMKII-30 retinas showed some differences. Plus retinas contained 54.8% of labeled area whereas the minus samples were 59.4%, exhibiting a 5% difference.

Retinal morphology at 8 days post light treatment. Normal, control rat retinas which have not been subjected to light treatment have an outer nuclear layer (ONL) that is usually about 10 nuclei thick. These are the cell bodies of the photoreceptors. When photoreceptors die and are removed, this layer becomes thinner, making it possible to estimate the extent of the damage from analysis of the ONL. Notice in **figure 11** that the photoreceptors make up about half the volume of the retina.

Following 5 hr of light treatment, photoreceptor DNA becomes fragmented. When this is extensive enough, those cells become apoptotic and die. Once removed they are not regenerated. **Figure 12** illustrates the retinal condition near the central portion of the light damaged portion. Notice that the neural retina (everything below the photoreceptors) is intact and appears normal. However, all photoreceptors have been lost. This is

extensive, and only at the periphery of the severe light damage are there a few cell bodies. These increase with distance toward the inferior edge. A region near the edge of the severely damaged area is shown in **figure 13**. Notable in this section are the reduced outer and inner segments and the dropout of some of the RPE cells. Notice also a normal neural retina and an ONL that is reduced to 5 cells thickness (about 50% reduction).

In all retinas studied at 8 days, form both lines of animals, there were regions of cell loss. These regions were centered on the superior portion of the retina. However, the NSE-45 retinas had only a narrow region of cell loss, while the CAMKII-30 animals demonstrated total loss for most of the superior retina, and sometimes into the inferior portion as well. It now appears that there is good correlation between the 24 hr TUNEL profile and the 8 day morphological study in that both demonstrate a very light sensitive region in the superior retina. However, TUNEL labeling appears to be slightly larger than the region of cell loss seen at 8 days, perhaps suggesting that some of the peripheral cells are not damaged sufficiently and, hence, are able to recover.

The effect of light on COX-2, bcl-2, bcl-K_L, and cytochrome-c levels. After dark adapted Sprague Dawley rats were exposed to 3 hours of light, they were kept in darkness for 5 or 21 hr (8 hr and 24 hr total experimental time). Under these conditions, using Western blot analysis, COX-2 levels were found to be increased more than two fold at both 8 and 24 hr. However, if animals were injected i.p. with the PAF receptor antagonist BN-50730 (30 mg/kg), significant inhibition was found for COX-2 protein levels (**figure 14**). Under these same conditions, bcl-2 protein levels were reduced to 30% of control levels at 8 hours and 65% at 24 hours (**figure 15**). Pretreatment with BN-50730 at both 8 and 24 hours significantly reduced the bcl-2 protein decrease in retinas of light treated animals. When bcl-X_L

protein was studied, there was also a significant drop in protein levels at 8 and 24 hr, but BN-50730 did not affect protein changes as observed in the bcl-2 study (**figure 16**). Finally, using the same experimental design as above, cytochrome-c levels were analyzed. Light treatment caused a significant increase at 8 hr but had little effect by 24 hr. Pretreatment with BN-50730 inhibited the increase in cytochrome-c (**figure 17**).

5 SUMMARY AND CONCLUSIONS

We have shown that light-induced formation of PAF leads to induction of COX-2, apoptosis, and photorecepotor cell death, and, therefore, reason that faster metabolism of PAF by PAF-AH could result in some level of protection for the retina. Hence, we have developed two lines of transgenic rats, each overexpressing a subunit of PAF-AH. One, the β regulatory subunit, is associated with the NSE promotor, the other, the α2 catalytic subunit, is under the direction of the CAMKII promotor. Litter mates, both plus and minus for these genes, were treated with 5 hr of light followed by 24 hr or 8 days of darkness. DNA fragmentation was analyzed after 24 hr; the extent of cell dropout was determined after 8 days.

DNA fragmentation in photoreceptors was 3 times more extensive, both in degree and area of retina, in the litter mates associated with the CAMKII-30 catalytic subunit of PAF-AH than in the NSE-45 regulatory subunit group. Interestingly, within the CAMKII-30 group, those retinas expressing the catalytic subunit appeared to have a smaller region of retina damaged, suggesting that the catalytic subunit may be somewhat involved in enhancing PAF metabolism. Conversely, there was no difference between the plus and minus retinas in the NSE-45 group.

Finally, the overall level of damage is far less within the NSE-45 retinas in

general. With a sample size of three animals in each condition, nothing can yet be determined, but it appears that the litter mates of the NSE-45 group are better protected than those of the CAMKII-30 group.

These initial observations are mirrored in the long term, 8 day dropout studies. The region of damage is far less in the NSE-45 retinas than in the CAMKII-30 samples, but at this time, we can not tell if the extent varies within the CAMKII-30 groups.

At present, we are comparing these animals, as well as additional animals from similar litters, to controls, to exactly determine the effects that these subunits have on the retina. In addition, we are now beginning to test combinations of these subunits to learn if protection can be enhanced. We are shortening the duration of the stimulus to achieve less damage so that it will be easier to determine the percent effect from each treatment, and we are mapping cell loss profiles in the 8 day animals. These graphs will then be superimposed on the 24 hr TUNEL plots to determine the percent of total damaged cells that are able to repair themselves.

In our studies on the effect of light treatment on the mitochondrial system, we found sharp declines in both bcl-2 and bcl-X_L protein levels following light damage. However, when animals where pretreated with the PAF receptor antagonist BN-50730, only the bcl-2 levels were affected; no changes were apparent in the bcl-X_L levels. This indicates that these two proteins share different regulatory pathways, and that the initial increase in PAF levels, following light treatment, only affects bcl-2. The increase in cytochrome-c levels after bright light, shown by Western blot, and its inhibition by the PAF antagonist, follows, strongly suggesting that increased levels of PAF may trigger mitochondrial-regulated apoptosis of photoreceptors.

In our experimental procedure, whole retinas were utilized for the Western blot analysis of cytochrome-c levels, so it is not yet known if the light induced up-regulation of cytochrome-c is a result of a mitochondrial response. We are currently repeating these experiments, but separating mitochondria from the rest of the retina prior to analysis to compare levels of mitochondrial and cytoplasmic cytochrome-c before and after light treatment. However, the protective effect of BN-50730, as shown in this portion of our study, correlates well with observations made earlier in this project, and again, strongly indicates that this compound is able to reduce or prevent DNA fragmentation and cell loss of photoreceptors after prolonged or extremely intense light treatment.

6 ABSTRACTS AND PUBLICATIONS

7 REFERENCES

Bazan NG, Fletcher BS, Herschman HR, Mukherjee PK. Platelet-activating factor and retinoic acid synergistically activate the inducible prostaglandin synthase gene. Proc Natl Acad Sci USA. 91: 5252-5256 (1994).

Bazan NG, Allan G, Marcheselli VL. An inhibitor of injury-induced COX-2 transcriptional activation elicits neuroprotection in a brain damage model. In: *Improved Non-steroid Anti-inflammatory Drugs; COX-2 Enzyme Inhibitors.* Vane J, Botting L, Botting R (Eds). Pp 145-166. Kluwer Academic Publishers: Lancester, United Kingdom (1996).

Coffey RJ, Hawkey CJ, Damstrup L, Graves-Deal R, Daniel VC, Dempsey PJ, Chinery R, Kirkland SC, DuBois RN, Jetton TL, Morrow JD. Epidermal growth factor receptor activation induces nuclear targeting of cyclooxygenase-2, basolateral release of prostaglandins, and mitogenesis in polarizing colon cancer cells. Proc Natl Acad Sci, USA. 94: 657-662 (1997).

Duckett CS, Li F, Wang Y, Tomaselli KJ, Thompson CB, Armstrong RC. Human IAP-like protein regulates programmed cell death downstream of Bcl-X_L and cytochrome c. Mol Cell Biol. 18:608-615 (1998).

Kaufmann WE, Worley PF, Pegg J, Bremer M, Isakson P. COX-2, a synaptically induced enzyme, is expressed by excitatory neurons at postsynaptic sites in rat cerebral cortex. Proc Natl Acad Sci, USA. 93: 2317-2321 (1996).

Kitamura Y, Shimohama S, Kamoshima W, Ota T, Matsuoka Y, Nomura Y, Smith MA, Perry G, Whitehouse PJ, Taniguchi T. Alteration of proteins regulating apoptosis, Bcl-2, Bcl-x, Bax, Bak, Bad, ICH-1, and CPP32, in Alzheimer's disease. Brain Res. 780:260-269 (1998).

Marcheselli VL, Bazan NG. Sustained induction of prostaglandin endoperoxide synthase-2 by seizures in hippocampus. Inhibition by a platelet-activating factor antagonist. J Biol Chem. 271: 24794-24799 (1996).

Miettinen S, Fusco FR, Yrjanheikki J, Keinanen R, Hirvonen T, Roivainen R, Narhi M, Hokfelt T, Koistinaho J. Spreading depression and focal brain ischemia induce cyclooxygenase-2 in cortical neurons through N-methyl-D-aspartic acid-receptors and phospholipase A_2. Proc Natl Acad Sci, USA. 94: 6500-6505 (1997).

Morita I, Schindler M, Regier MK, Otto JC, Hori T, DeWitt DL, Smith WL. Different intracellular locations for prostaglandin endoperoxide H synthase-1 and -2. J Biol Chem. 270:10902-10908 (1995).

Oberhammer F, Wilson JW, Dive C, Morris ID, Wakeling AE, Walker PR. Sikorska M. Apoptotic death in epithelial cells: cleavage of DNA to 300 and/or 50 kb fragments prior to or in the absence of internucleosomal fragmentation. EMBO J. 12:3679-3684 (1993).

Rossé T, Olivier R, Monney L, Rager M, Conus S, Fellay I, Jansen B, Borner C. Bcl-2 prolongs cell survival after Bax-induced release of cytochrome c. Nature. 391:496-499 (1998).

Schulze-Osthoff K, Bakker AC, Vanhaesebroeck B, Beyaert R, Jacob WA, Fiers W. Cytotoxic activity of tumor necrosis factor is mediated by early damage of mitochondrial functions. Evidence for the involvement of mitochondrial radical generation. J Biol Chem. 267:5317-5323 (1992).

Yamagata K, Andreasson KI, Kaufmann WE, Barnes CA, Worley PF. Expression of a mitogen-inducible cyclooxygenase in brain neurons: Regulation by synaptic activity and glucocorticoids. Neuron. 11:371-386 (1993).

Zou H, Henzel WJ, Liu X, Lutschg A, Wang X. Apaf-1, a human protein homologous to *C. elegans* CED-4, participates in cytochrome c-dependent activation of caspase-3. Cell. 90:405-413 (1997).

Figure 1

OVEREXPRESSION OF THE β (45kDa) SUBUNIT UNDER THE DIRECTION OF THE NSE PROMOTOR

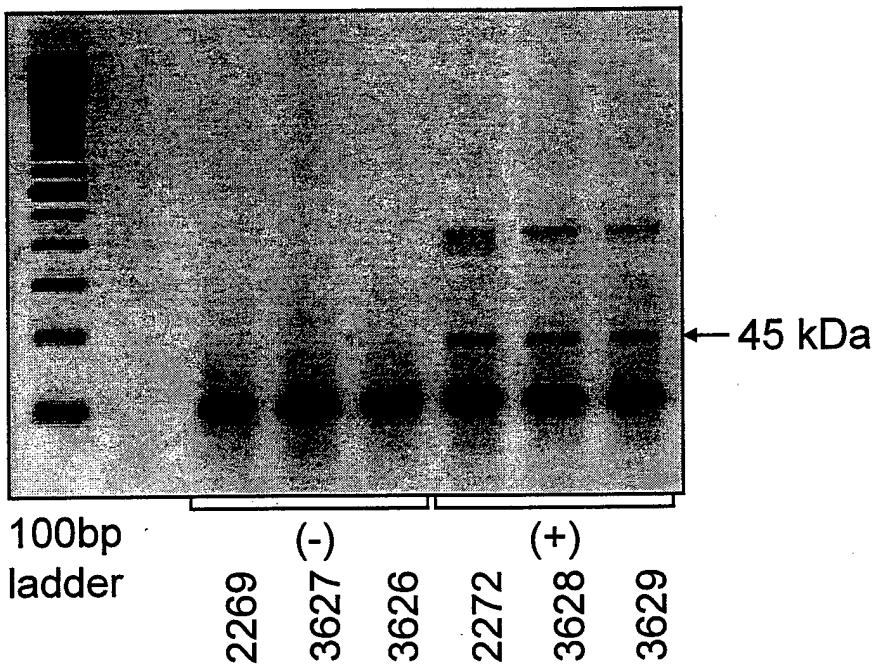

RT-PCR gel demonstrating the presence (+) or absence (-) of the NSE promotor-associated β (45 kDa) regulatory subunit. Reverse transcriptase polymerase chain reaction (RT-PCR) was done to indicate which of the transgenic PAF-AH subunit sequences were expressed. PCR was done with 2.0 µl of first strand cDNA samples, 400nM primers, 1.5mM Mgcl, 0.1mM dNTPs, 0.5 units of Taq DNA polymerase, and 1x PCR buffer in a final volume of 25 µl. Amplification for both the α2 (30 kDa) and β (45 kDa) subunits was for 30 cycles (94°C for 0.25 minutes, 60°C for 0.25 minutes, and 72°C for 0.5 minutes). The PCR products were electrophoresed in a 1.8% agarose gel and stained with ethidium bromide. Animal ear tag numbers are indicated below each lane. The 100 bp ladder at the left serves as a size reference.

Figure 2

OVEREXPRESSION OF THE α 2 (30 kDa) SUBUNIT UNDER THE DIRECTION OF THE CAMK11 PROMOTOR

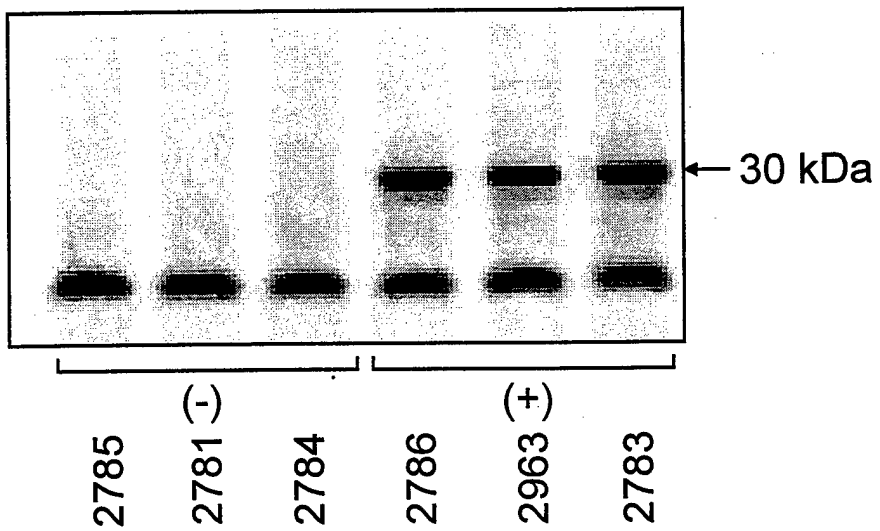

RT-PCR gel demonstrating the presence (+) or absence (-) of the CAMKII promotor-associated α2 (30 kDa) catalytic subunit. Reverse transcriptase polymerase chain reaction (RT-PCR) was done to indicate which of the transgenic PAF-AH subunit sequences were expressed. PCR was done with 2.0 µl of first strand cDNA samples, 400nM primers, 1.5mM Mgcl, 0.1mM dNTPs, 0.5 units of Taq DNA polymerase, and 1x PCR buffer in a final volume of 25 µl. Amplification for both the α2 (30 kDa) and β (45 kDa) subunits was for 30 cycles (94°C for 0.25 minutes, 60°C for 0.25 minutes, and 72°C for 0.5 minutes). The PCR products were electrophoresed in a 1.8% agarose gel and stained with ethidium bromide. Animal ear tag numbers are indicated below each lane.

Figure 3

Light micrograph, fluorescence microscopy, demonstrating the typical TUNEL labeling pattern in NSE-45 transgenic rat retinas. Fragmented DNA fluoresces bright yellow with an FITC label. For better orientation, all nuclei are labeled with propidium iodide which lightly fluoresces red. Photoreceptor outer segments are oriented up; vitreal surface is down. Both NSE-45 + and - TUNEL label in similar patterns. This transgenic line labels only modestly after 5 hours of light treatment plus 19 hours. Notice that only photoreceptor nuclei are TUNEL labeled (outer nuclear layer). Original microscope magnification, 400 X.

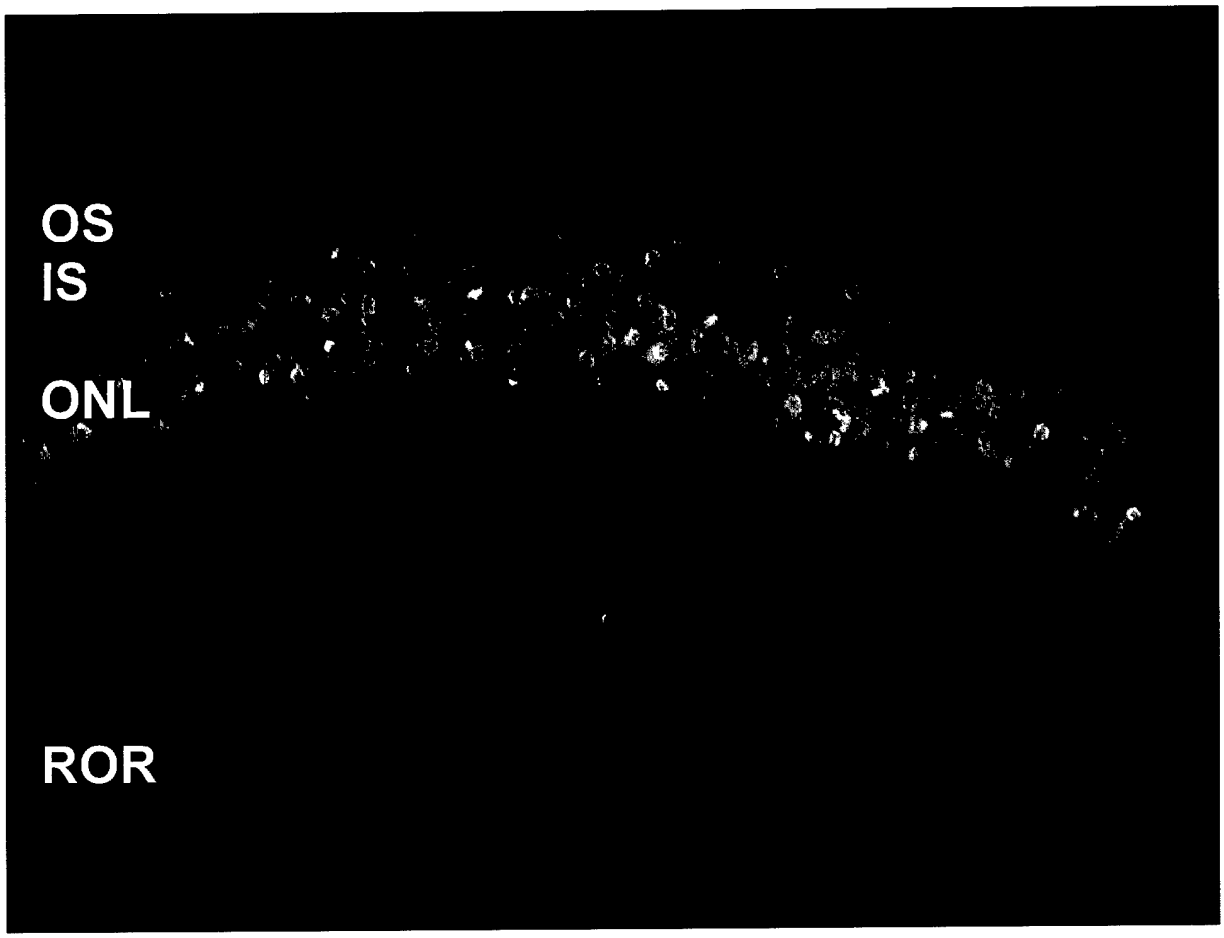
OS
IS
ONL
ROR

Figure 4

Light micrograph, fluorescence microscopy, illustrating a typical TUNEL labeling pattern in the CAMKII-30 transgenic rat retina. Fragmented DNA fluoresces bright yellow. All retinal nuclei are labeled with propidium iodide which lightly fluoresces red. Photoreceptor outer segments are oriented up; vitreal surface is down. Both the CAMKII-30 + and - TUNEL label intensely, generally in similar patterns. However, the area of the label is more extensive in the CAMKII-30 minus animals. This transgenic line labels only modestly after 5 hours of light treatment plus 19 hours. Again, notice that only photoreceptor nuclei are TUNEL labeled (outer nuclear layer). Original microscope magnification, 400 X.


RPE

Figure 6

Data table listing light values for each of the 33 retinal fields, for each of the rats. Field 1, superior edge; field 33, inferior edge. The two blank fields 16 and 17 in animal 2781 represent the optic nerve. The light from each 400 X microscope field was measured with an automatic metering system and the length of time (sec) for the correct exposure was recorded. Thus, high TUNEL labeling produced a small number, low or no label resulted in a large number. When plotted linearly as a histogram, the resulting profile represented the extent of label across the retina (**figures 8** and **9**). The gray areas in each column are fields that contained no TUNEL label. For each animal, these were averaged to obtain a background level to which the rest of the fields could be compared. These averages are indicated at the bottom of each column. These averages were defined as 100% (**figure 7**). Animal ear tag numbers are indicated at the top of each column.

		NSE						CAMKII					
		2269 -	3626 -	3627 -	3629 +	2272 +	3628 +	2785 -	2781 -	2784 -	2786 +	2963 +	2783 +
1		47.9	39.8	23.4	21.9	25.7	61.7	91.21	12.9	97.7	28.18	19.1	#N/A
2		33.9	39.8	23.4	20.0	24.6	47.9	28.18	6.3	52.5	32.36	10.7	10.7
3		35.5	39.8	20.0	19.1	25.7	56.2	14.13	7.2	29.5	45.71	9.3	9.3
4		28.2	32.4	20.9	20.9	20.4	57.6	15.85	8.7	25.7	64.57	11.8	12.9
5		28.8	29.5	20.9	21.9	23.4	47.9	10.72	8.5	22.9	64.57	10.2	9.8
6		16.6	24.6	20.9	20.0	25.7	50.1	9.77	8.0	15.1	54.96	10.2	10.7
7		19.1	26.9	20.9	20.9	20.9	38.0	14.13	8.7	12.9	60.26	8.7	11.8
8		29.5	41.7	17.8	18.2	13.5	29.5	9.33	8.3	12.9	64.57	12.0	18.2
9		38.0	39.8	14.5	15.9	10.7	28.2	7.94	14.1	14.1	64.57	15.9	13.5
10		28.2	43.7	15.1	14.8	8.9	21.9	9.33	22.9	11.2	64.57	12.9	15.9
11		38.0	33.9	20.9	10.7	11.5	39.8	13.49	10.2	19.1	70.79	16.6	19.1
12		35.5	41.7	16.6	17.4	10.7	52.5	12.88	12.9	57.6	64.57	16.6	16.6
13		32.4	38.0	23.4	18.2	13.5	50.1	13.49	11.8	125.9	77.63	11.2	15.9
14		38.0	34.7	20.0	23.4	18.2	52.5	14.13	12.3	114.8	85.11	14.1	10.2
15		38.0	39.8	21.4	33.9	19.1	66.1	12.3	8.3	104.7	57.55	12.9	11.8
16		33.9	38.9	24.6	30.9	17.4	55.0	13.49	#N/A	104.7	54.96	15.9	12.3
17		39.8	35.5	21.9	30.2	15.9	43.7	8.71	#N/A	125.9	60.26	21.9	11.2
18		45.7	28.2	19.1	23.4	29.5	50.1	10.23	11.8	120.2	#N/A	19.1	12.3
19		47.9	23.4	17.4	23.4	28.2	47.9	9.33	10.7	134.9	74.14	29.5	21.9
20		47.9	25.7	26.9	24.6	30.9	50.1	10.23	10.7	141.3	#N/A	52.5	55.0
21		43.9	35.5	23.4	20.9	39.4	57.6	10.72	9.8	141.3	#N/A	60.3	85.1
22		52.5	37.2	24.0	23.4	38.0	#N/A	7.58	15.1	218.8	#N/A	64.6	74.1
23		55.0	43.7	28.0	20.9	33.9	#N/A	9.77	35.5	204.2	81.29	60.3	89.1
24		47.9	#N/A	28.2	18.2	26.9	#N/A	9.77	55.0	204.2	81.29	67.6	74.1
25		43.7	#N/A	28.0	20.0	28.2	#N/A	11.22	57.6	204.2	70.79	64.6	70.8
26		43.7	#N/A	25.7	20.9	28.2	#N/A	22.91	55.0	#N/A	70.79	60.3	97.7
27		50.1	#N/A	23.4	29.5	26.9	#N/A	39.81	57.6	#N/A	64.57	64.6	81.3
28		41.7	#N/A	21.9	28.2	26.9	#N/A	45.71	60.3	#N/A	70.79	64.6	109.7
29		38.0	#N/A	#N/A	23.4	25.7	#N/A	47.86	70.8	#N/A	77.63	67.6	110.0
30		43.7	#N/A	#N/A	#N/A	28.2	#N/A	47.86	#N/A	#N/A	#N/A	64.6	110.0
31		45.7	#N/A	#N/A	#N/A	29.5	#N/A	50.12	#N/A	#N/A	#N/A	60.3	110.0
32		45.7	#N/A	#N/A	#N/A	28.2	#N/A	#N/A	#N/A	#N/A	#N/A	60.3	67.6
33		56.2	#N/A	#N/A	#N/A	26.9	#N/A	#N/A	#N/A	#N/A	#N/A	#N/A	93.3
	100%	46.8	38.8	25.5	27.0	28.1	51.4	48.6	59.3	207.9	74.2	63.3	97.5

Figure 7

Normalized data sheet obtained by converting field values from figure 6 to percentages of each animal's averaged background.

	Nomalized TO % values											
		NSE						CAMKII					
		2269 -	3626 -	3627 -	3629 +	2272 +	3628 +	2785 -	2781 -	2784 -	BAD	2963 +	2783 +
1		102.2	102.7	91.9	80.9	91.4	119.9	58.0	21.7	47.0		30.1	11.0
2		72.4	102.7	91.9	73.8	87.3	93.1	58.0	10.6	25.2		16.9	11.0
3		75.8	102.7	78.2	70.5	91.4	109.4	29.1	12.2	14.2		14.7	9.6
4		60.2	83.5	81.9	77.2	72.6	111.9	32.6	14.7	12.4		18.6	13.2
5		61.6	76.1	81.9	80.9	83.3	93.1	22.1	14.5	11.0		16.2	10.0
6		35.5	63.3	81.9	73.8	91.4	97.5	20.1	14.0	7.3		16.2	11.0
7		40.7	69.4	81.9	77.2	74.3	74.0	29.1	14.7	6.2		13.8	12.1
8		63.0	107.6	69.7	67.3	48.0	57.4	19.2	14.0	6.2		19.0	18.7
9		81.2	102.7	56.7	58.6	38.1	54.8	16.3	23.8	6.8		25.0	13.8
10		60.2	112.6	59.4	54.7	31.7	42.6	19.2	38.6	5.4		20.4	16.3
11		81.2	87.4	81.9	39.6	40.8	77.4	27.7	17.2	9.2		26.2	19.6
12		75.8	107.6	65.1	64.3	38.1	102.1	26.5	21.7	27.7		26.2	17.0
13		69.1	98.1	91.9	67.3	48.0	97.5	27.7	19.8	60.6		17.7	16.3
14		81.2	89.4	78.2	86.7	64.7	102.1	29.1	20.7	55.2		22.3	10.5
15		81.2	102.7	83.8	125.3	67.8	105.0	25.3	14.0	50.4		20.4	12.1
16		72.4	100.4	96.3	114.3	61.8	106.9	27.7	OPTIC	50.4		25.0	12.6
17		85.0	91.5	85.8	111.7	56.3	84.9	17.9	NERVE	60.6		34.6	11.5
18		97.6	72.7	74.7	86.7	104.9	97.5	21.0	19.8	57.8		30.1	12.6
19		102.2	60.5	68.1	86.7	100.2	93.1	19.2	18.1	64.9		46.6	22.5
20		102.2	66.3	105.5	90.8	109.8	97.5	21.0	18.1	68.0		82.9	56.4
21		93.7	91.5	91.9	77.2	140.0	111.9	22.1	16.5	68.0		95.2	87.3
22		112.1	95.8	94.1	86.7	135.1	#N/A	15.6	25.5	105.3		102.0	76.1
23		117.4	112.6	100.0	77.2	120.4	#N/A	20.1	59.8	98.2		95.2	91.5
24		102.2	#N/A	110.5	67.3	95.7	#N/A	20.1	92.6	98.2		106.8	76.1
25		93.2	#N/A	100.0	73.8	100.2	#N/A	23.1	97.0	98.2		102.0	72.6
26		93.2	#N/A	100.8	77.2	100.2	#N/A	47.1	92.6	#N/A		95.2	100.3
27		107.1	#N/A	91.9	109.1	95.7	#N/A	81.9	97.0	#N/A		102.0	83.4
28		89.1	#N/A	85.8	104.2	95.7	#N/A	94.0	101.5	#N/A		102.0	112.6
29		81.2	#N/A	#N/A	86.7	91.4	#N/A	98.5	119.3	#N/A		106.8	112.9
30		93.2	#N/A	#N/A	#N/A	100.2	#N/A	98.5	#N/A	#N/A		102.0	112.9
31		97.6	#N/A	#N/A	#N/A	104.9	#N/A	#N/A	#N/A	#N/A		95.2	112.9
32		97.6	#N/A	#N/A	#N/A	100.2	#N/A	#N/A	#N/A	#N/A		95.2	69.4
33		120.1	#N/A	#N/A	#N/A	95.7	#N/A	#N/A	#N/A	#N/A		#N/A	95.8

Figure 8

TUNEL- LABELING IN NSE-45 TRANSGENIC RAT RETINAS

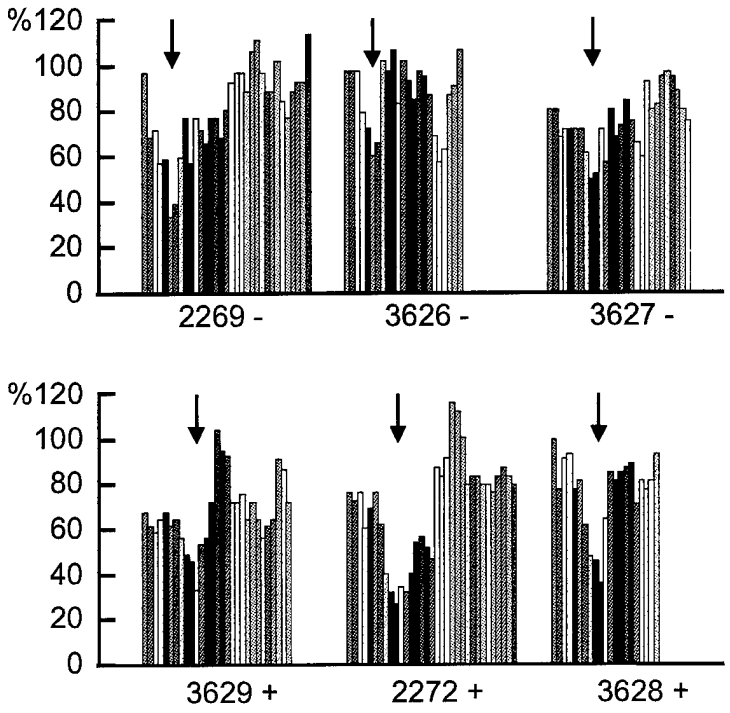

Retinal plot demonstrating the extent of TUNEL labeling in the NSE-45 plus and minus transgenic rats. Each histogram represents one retina with the upper (superior) edge to the left and the lower (inferior) retinal margin to the right. These plots are inverse light measurements; i.e., the stronger the light (the more TUNEL fluorescence present) in a particular field, the shorter the bar. These animals all demonstrate a largely dark retina with a small region damaged by light (arrows). Generally, there are no differences between the two groups. Animal ear tag numbers are indicated below each plot.

Figure 9

TUNEL- LABELING IN CAMKII-30 TRANSGENIC RAT RETINAS

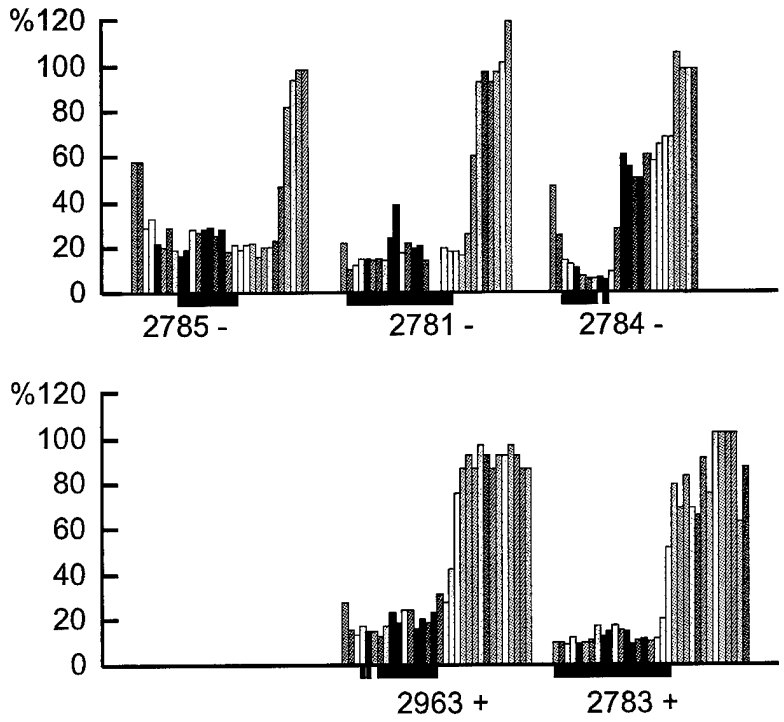

Retinal plot demonstrating the extent of TUNEL labeling in the CAMKII-30 plus and minus transgenic rats. As above, each histogram represents one retina with the upper (superior) edge to the left and the lower (inferior) retinal margin to the right. These animals are extensively damaged, as shown by the broad short region centered on the upper half of the retina. Although both the plus and minus rats show this damage, the width of the damage is significantly less in the two plus animals. Unlike the NSE-45 rat retinas (figure 8), these all had a highly labeled region of RPE cells centered in the area of photoreceptor damage. The position of these areas is indicated by the horizontal bar below each retinal plot. Animal ear tag numbers are indicated as well.

Figure 10

Comparison of TUNEL-labeled regions within each retina. The total possible quantity for each retinal field is 100; the total number of fields is 30. Thus, the total possible unlabeled "area" for each retina is 3000. The presence of any TUNEL label will reduce this amount. Subtracting the measured field value from 100 gives the amount of TUNEL label present within each field. These values are listed here for each field, for each retina. The sum of these fields is indicated at the bottom of the column. The percent damage is obtained when this number is taken as a percentage of 3000. The percent damage for all animals within a treatment was averaged to get mean percent damage for each treatment; that is, plus and minus NSE-45 and plus and minus CAMKII-30. The CAMKII-30 animals were more than 3 times affected by light than the NSE-45 animals. NSE-45 plus and minus animals, however, showed no differences, but there was a slight trend within the CAMKII-30 animals for the plus animals to be slightly less affected by light.

	NSE							CAMK				
SECTION #	2269 -	3626 -	3627 -	3629 +	2272 +	3628 +	SECTION #	2785 -	2781 -	2784 -	2963 +	2783 +
1			-15	-19	-9		1	-42	-78	-53	-70	-89
2	-28		-15	-26	-13	-7	2	-42	-89	-75	-83	-89
3	-24		-28	-30	-9		3	-71	-88	-86	-85	-90
4	-40	-17	-24	-23	-27		4	-67	-85	-88	-81	-87
5	-38	-24	-24	-19	-17	-7	5	-78	-86	-89	-84	-90
6	-65	-37	-24	-26	-9	-3	6	-80	-86	-93	-84	-89
7	-59	-31	-24	-23	-26	-26	7	-71	-85	-94	-86	-88
8	-37		-35	-33	-52	-43	8	-81	-86	-94	-81	-81
9	-19		-48	-41	-62	-45	9	-84	-76	-93	-75	-86
10	-40		-45	-45	-68	-57	10	-81	-61	-95	-80	-84
11	-19	-13	-24	-60	-59	-23	11	-72	-83	-91	-74	-80
12	-24		-40	-36	-62		12	-74	-78	-72	-74	-83
13	-31	-2	-15	-33	-52	-3	13	-72	-80	-39	-82	-84
14	-19	-11	-28	-13	-35		14	-71	-79	-45	-78	-90
15	-19		-22		-32		15	-75	-86	-50	-80	-88
16	-28		-11		-38		16	-72	OPTIC	-50	-75	-87
17	-15	-8	-21		-44	-15	17	-82	NERVE	-39	-65	-88
18	-2	-27	-31	-13		-3	18	-79	-80	-42	-70	-87
19		-40	-37	-13		-7	19	-81	-82	-35	-53	-78
20		-34	-2	-9		-3	20	-79	-82	-32	-17	-44
21	-6	-8	-15	-23			21	-78	-84	-32	-5	-13
22		-4	-13	-13			22	-84	-74	5		-24
23				-23			23	-80	-40	-2	-5	-9
24				-33	-4		24	-80	-7	-2		-24
25	-7			-26	0		25	-77	-3	-2		-27
26	-7		-7	-23	0		26	-53	-7		-5	
27	7		-15		-4		27	-18	-3			-17
28	-11		-21		-4		28	-6				
29	-19			-13	-9		29	-2				
30	-7						30	-2				
3000	-555	-254	-583	-617	-635	-240		-1932	-1691	-1386	-1491	-1795
% damaged	-18.5	-11.1	-20.8	-21.3	-21.2	-11.4		-64.4	-58.3	-55.4	-49.7	-59.8
mean	-16.8			-17.9				-59.4			-54.8	
sd	5.1			5.7				4.6			7.2	

Figure 11

Light micrograph showing a healthy rat retina that has not been subjected to 5 hr of light. Photoreceptors are oriented upward, vitreous is at the bottom. RPE, retinal pigment epithelium. OS, photoreceptor outer segments. IS, photoreceptor inner segments. ONL, outer nuclear layer - photoreceptor nuclei. ROR, rest of retina. Notice in this control retina that photoreceptors occupy approximately 50% of the retinal volume, and that in normal retinas, the ONL is usually about 10 nuclei thick. The vertical lines within the neural retina (region below the photoreceptors) are the Müller cell processes. Their presence indicates that the section is not oblique and that the thicknesses of the retinal layers are "true dimension". Original microscope magnification, 400 X.

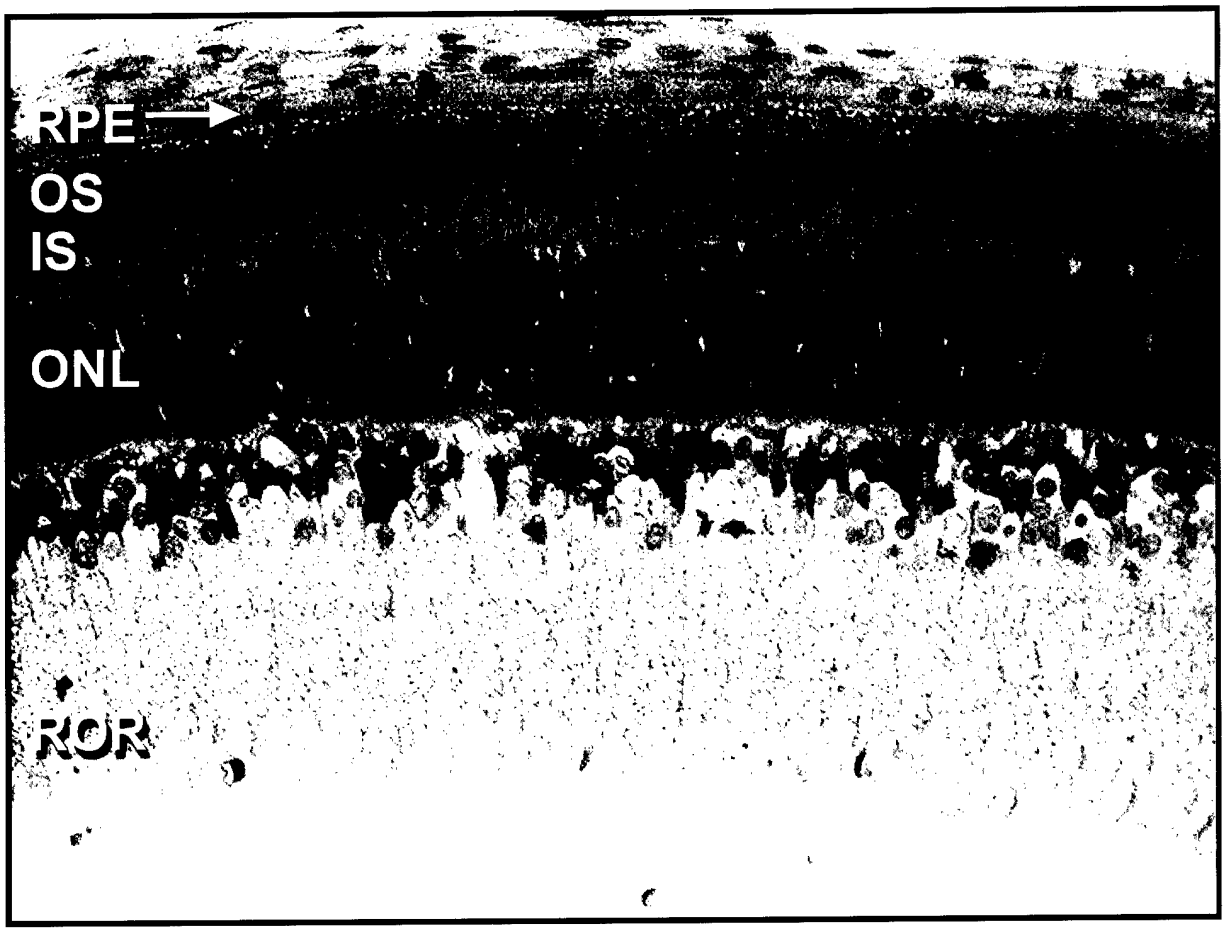
RPE
OS
IS
ONL
ROR

Figure 12

Light micrograph showing the central region of a 5 hr light damaged rat retina followed by 8 days of darkness. Orientation is as in **figure 11** with vitreous at the bottom. RPE, retinal pigment epithelium. ROR, rest of retina. Notice here that all photoreceptors have been lost, leaving only the intact ROR. There is also some internal damage to the RPE, as shown by occasional regions of vesiculated cytoplasm. Original microscope magnification, 400 X.

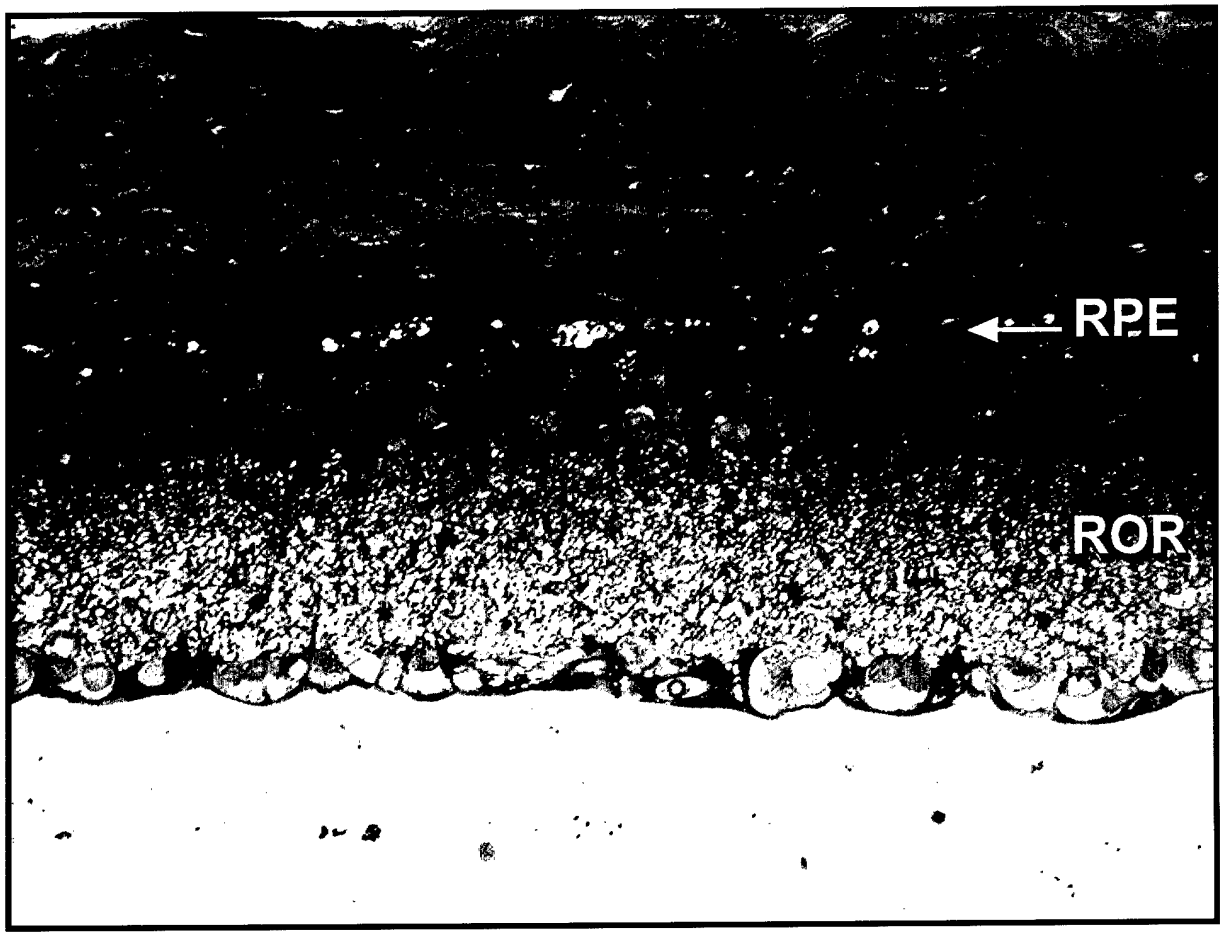
RPE
ROR

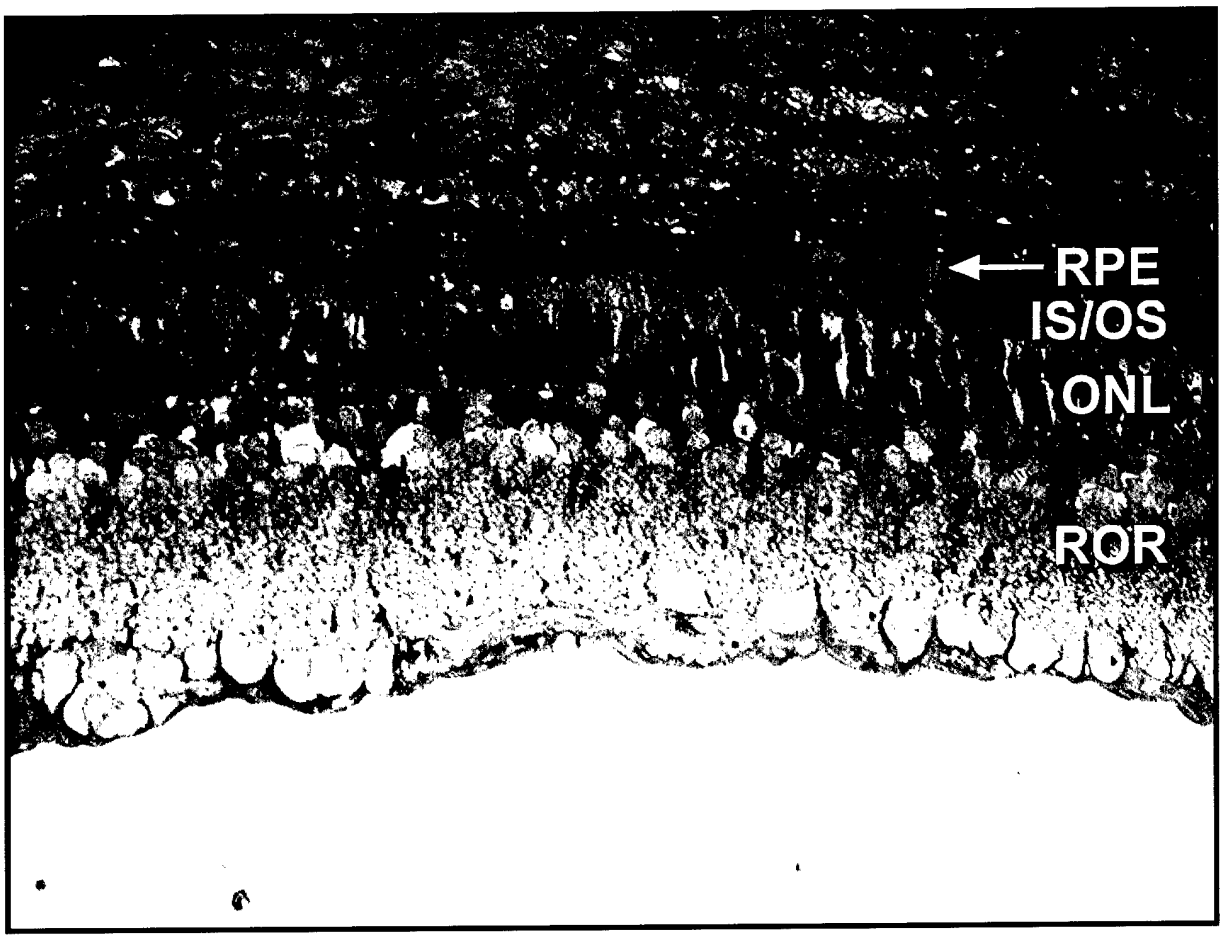
RPE
IS/OS
ONL
ROR

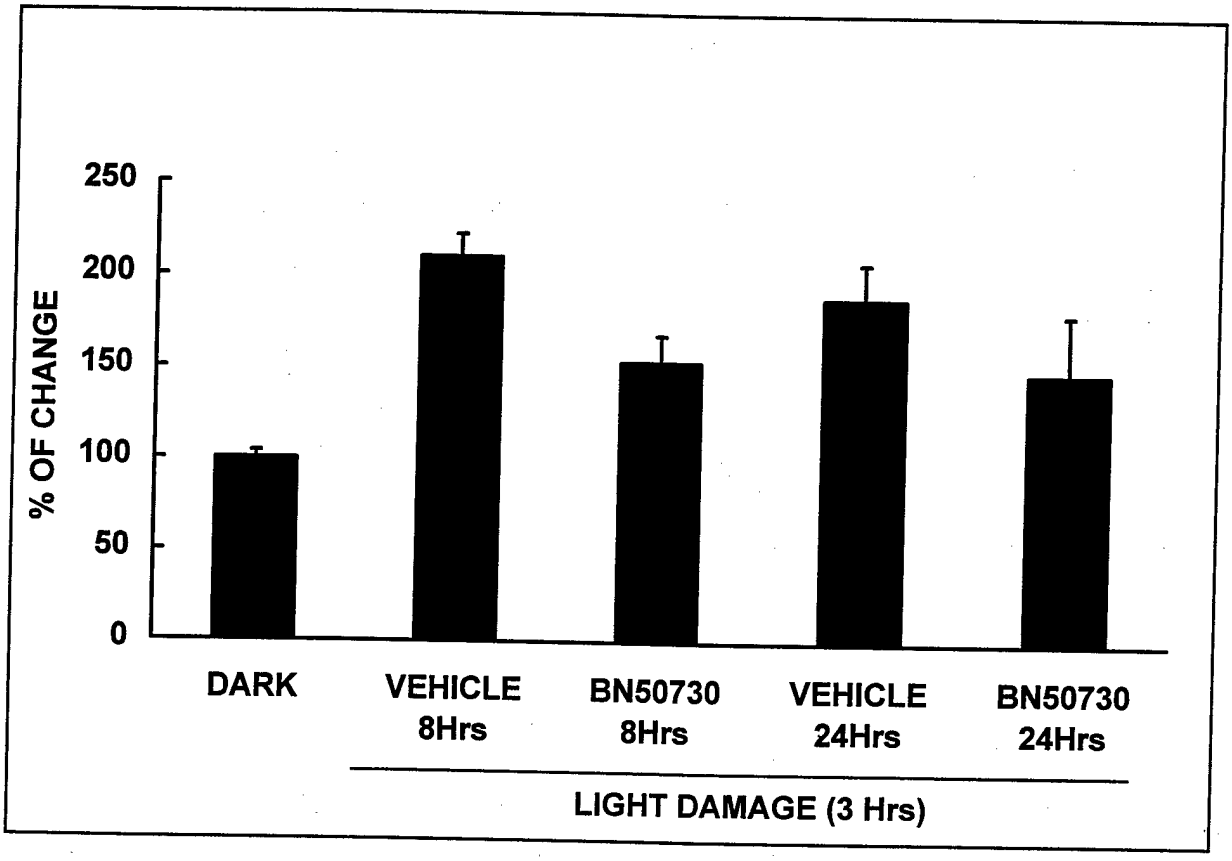

Figure 14

Percent distribution of COX-2 protein levels in rat retina after 3 hours of light damage. After light exposure animals were kept in the dark for 8 and 24 hours. Retina homogenate was used for Western blot analysis. Data shown is the mean value ± SD from two experiments (n = 7 individual determinations).

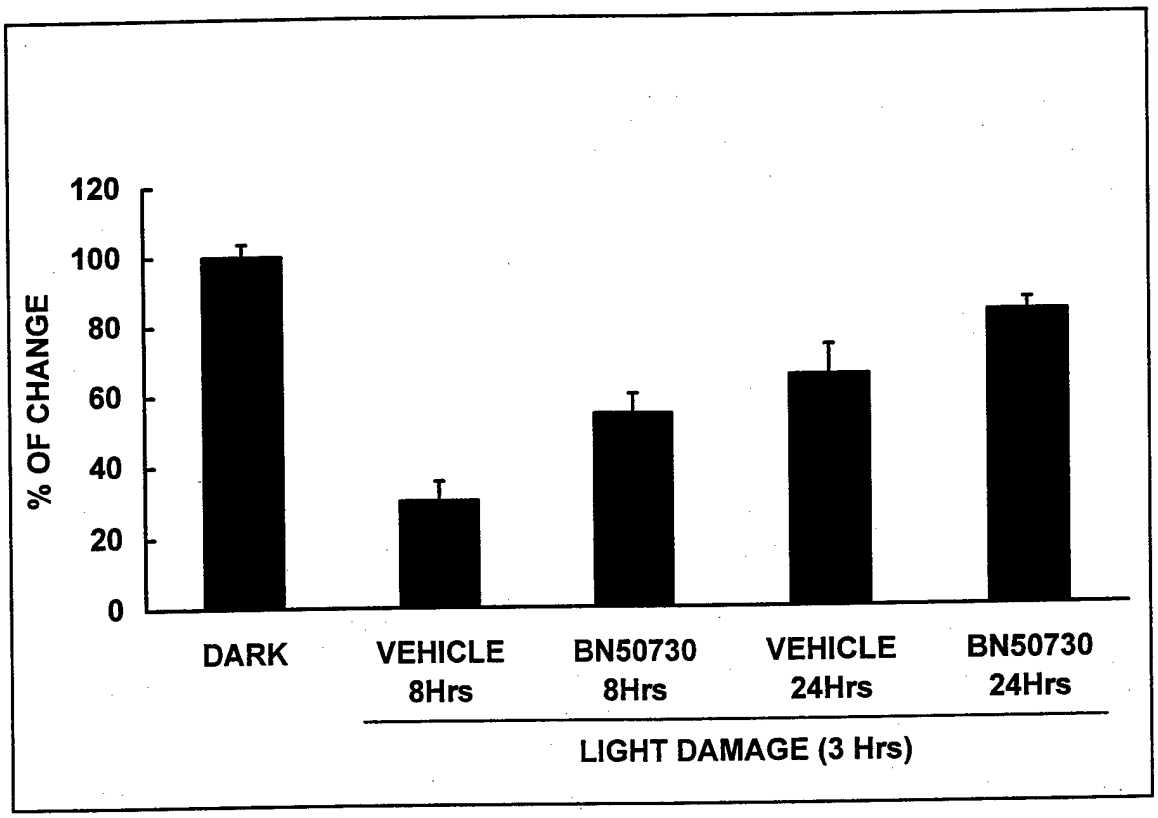

Figure 15

Percent distribution of bcl-2 protein levels in rat retina 3 hours after light damage. Effect of BN-50730. The drastic reduction of bcl-2 protein measured 8 and 24 hours after 3 hours of light damage, was partially antagonized by BN-50730. When bcl-2 accumulates, it forms bcl-2 homodimers which, in turn, protect the cell from undergoing apoptosis.

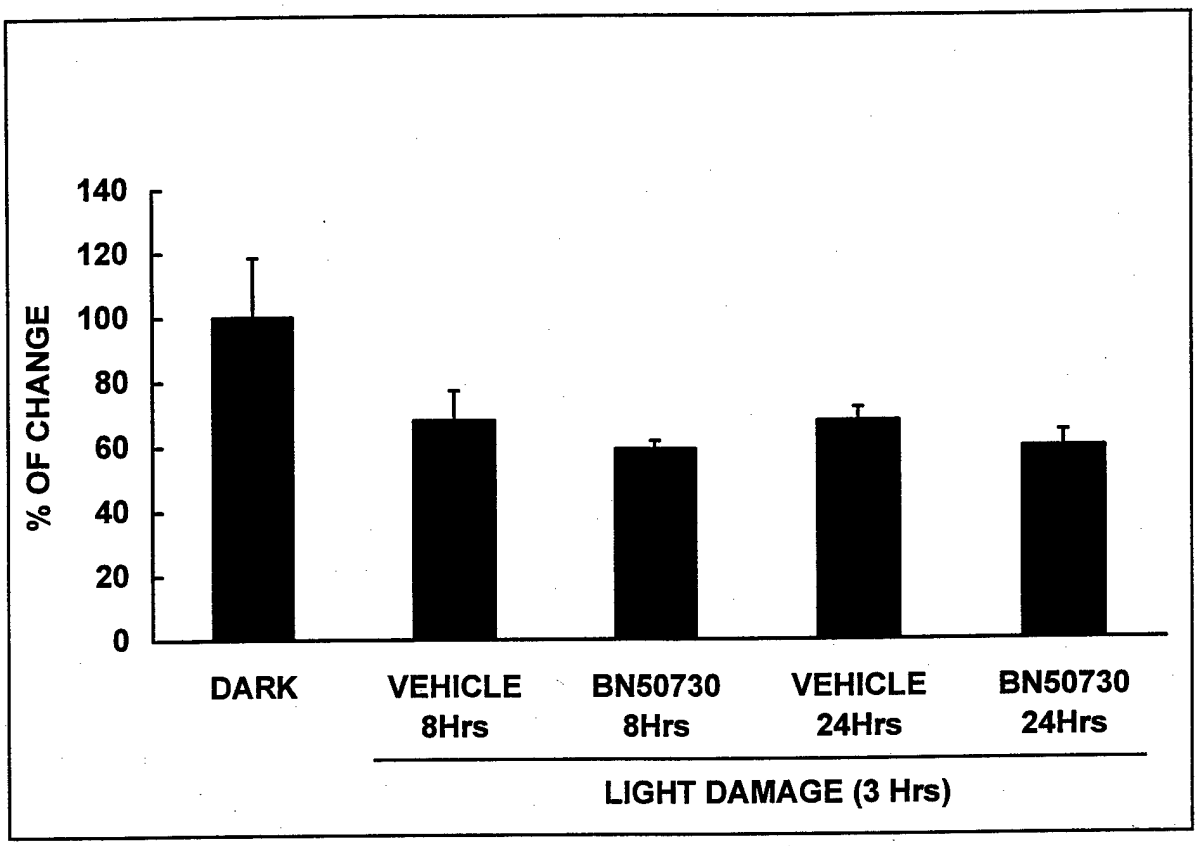

Figure 16

Percent distribution of bcl-xl protein levels in rat retina after 3 hours of light damage. Effect of BN- 50730. Details as in **figure 1** legend.

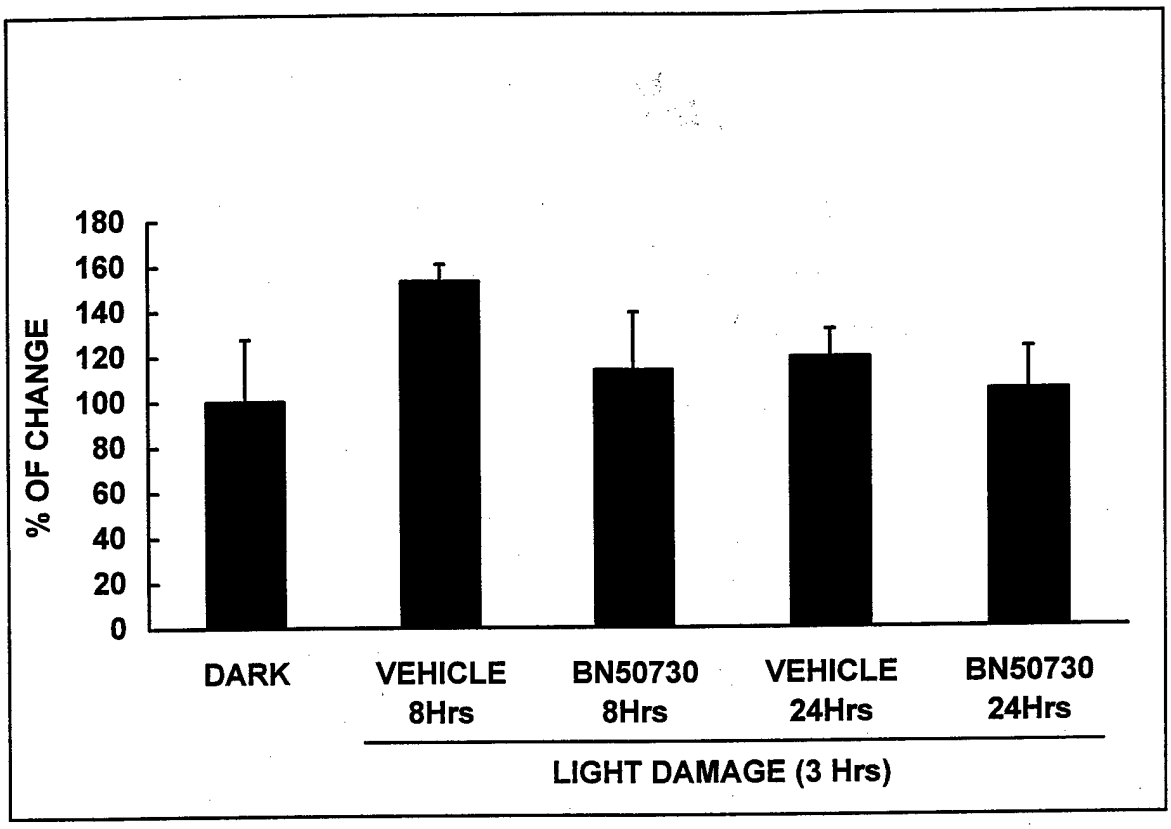

Figure 17

Percent distribution of cytochrome-c protein levels in rat retina after 3 hours of light damage. Effect of BN-50730. Details as in **figure 1** legend.